MAY 17 1930

VOLUME LXXI NUMBER 2

THE ASTROPHYSICAL JOURNAL

AN INTERNATIONAL REVIEW OF SPECTROSCOPY AND ASTRONOMICAL PHYSICS

Edited by

GEORGE E. HALE
Mount Wilson Observatory of the Carnegie Institution of Washington

EDWIN B. FROST
Yerkes Observatory of the University of Chicago

HENRY G. GALE
Ryerson Physical Laboratory of the University of Chicago

MARCH 1930

THE SPECTROHELIOSCOPE AND ITS WORK - - - *George E. Hale* 73

LUNAR RADIATION AND TEMPERATURES - - *Edison Pettit and Seth B. Nicholson* 102

PRELIMINARY RESULTS OF SPECTROGRAPHIC OBSERVATIONS OF 7ϵ AURIGAE *O. Struve and C. T. Elvey* 136

PHOSPHORUS IN STELLAR SPECTRA - - - - - *Otto Struve* 150

THE UNIVERSITY OF CHICAGO PRESS
CHICAGO, ILLINOIS, U.S.A.

March 1930 Vol. LXXI, No. 2

THE ASTROPHYSICAL JOURNAL

AN INTERNATIONAL REVIEW OF SPECTROSCOPY AND ASTRONOMICAL PHYSICS

Edited by

GEORGE E. HALE
Mount Wilson Observatory of the Carnegie Institution of Washington

EDWIN B. FROST
Yerkes Observatory of the University of Chicago

HENRY G. GALE
Ryerson Physical Laboratory of the University of Chicago

WITH THE COLLABORATION OF

WALTER S. ADAMS, Mount Wilson Observatory
JOSEPH S. AMES, Johns Hopkins University
ARISTARCH BELOPOLSKY, Observatoire de Pulkovo
WILLIAM W. CAMPBELL, Lick Observatory
HENRY CREW, Northwestern University
CHARLES FABRY, Université de Paris
ALFRED FOWLER, Imperial College, London
CHARLES S. HASTINGS, Yale University
HEINRICH KAYSER, Universität Bonn
ALBERT A. MICHELSON, University of Chicago
ROBERT A. MILLIKAN, Institute of Technology, Pasadena
HUGH F. NEWALL, Cambridge University
HENRY N. RUSSELL, Princeton University
FRANK SCHLESINGER, Yale Observatory
SIR ARTHUR SCHUSTER, Twyford
FREDERICK H. SEARES, Mount Wilson Observatory

The Astrophysical Journal is published by the University of Chicago at the University of Chicago Press, 5750 Ellis Avenue, Chicago, Illinois, during each month except February and August. ¶ The subscription price is $6.00 a year; the price of single copies is 75 cents. Orders for service of less than a half-year will be charged at the single-copy rate. ¶ Postage is prepaid by the publishers on all orders from the United States, Mexico, Cuba, Porto Rico, Panama Canal Zone, Republic of Panama, Dominican Republic, Canary Islands, El Salvador, Argentina, Bolivia, Brazil, Colombia, Chile, Costa Rica, Ecuador, Guatemala, Honduras, Nicaragua, Peru, Hayti, Uruguay, Paraguay, Hawaiian Islands, Philippine Islands, Guam, Samoan Islands, Balearic Islands, Spain, and Venezuela. ¶ Postage is charged extra as follows: for Canada and Newfoundland, 30 cents on annual subscriptions (total $6.30); on single copies, 3 cents (total 78 cents); for all other countries in the Postal Union, 50 cents on annual subscriptions (total $6.50), on single copies 5 cents (total 80 cents). ¶ Patrons are requested to make all remittances payable to The University of Chicago Press, in postal or express money orders or bank drafts.

The following are authorized agents:

For the British Empire, except North America, India, and Australasia: The Cambridge University Press, Fetter Lane, London, E.C. 4. Yearly subscriptions, including postage, £1 9*s*. 3*d*. each; single copies, including postage, 3*s*. 6*d*. each.

For Japan: The Maruzen Company, Ltd., Tokyo.

For China: The Commercial Press, Ltd., Paoshan Road, Shanghai. Yearly subscriptions, $6.00; single copies, 75 cents, or their equivalents in Chinese money. Postage extra, on yearly subscriptions 50 cents, on single copies 5 cents.

Claims for missing numbers should be made within the month following the regular month of publication. The publishers expect to supply missing numbers free only when losses have been sustained in transit, and when the reserve stock will permit.

Business Correspondence should be addressed to The University of Chicago Press, Chicago, Illinois.

Communications for the editors and manuscripts should be addressed to the Editors of THE ASTROPHYSICAL JOURNAL, Yerkes Observatory, Williams Bay, Wisconsin.

The cable address is "Observatory, Williamsbay, Wisconsin."

The articles in this Journal are indexed in the *International Index to Periodicals*, New York, N.Y.

Entered as second-class matter, January 17, 1895, at the Post-office at Chicago, Ill., under the act of March 3, 1879.
Acceptance for mailing at special rate of postage provided for in Section 1103, Act of October 3, 1917, authorized on July 25, 1918.

PRINTED IN THE U.S.A.

THE ASTROPHYSICAL JOURNAL

AN INTERNATIONAL REVIEW OF SPECTROSCOPY AND ASTRONOMICAL PHYSICS

VOLUME LXXI MARCH 1930 NUMBER 2

THE SPECTROHELIOSCOPE AND ITS WORK[1]

PART II. THE MOTIONS OF THE HYDROGEN FLOCCULI NEAR SUN-SPOTS

By GEORGE E. HALE

ABSTRACT

The purpose of this paper is to describe in detail some of the rapid motions of hydrogen flocculi near sun-spots. The observations, to be discussed in a future article of this series, were made visually by the author with a spectrohelioscope, which in certain respects is better adapted than other instruments for work of this nature.

In the first part of this paper[2] I have described some of the motions of hydrogen flocculi seen with the spectrohelioscope, without going into the details of many observations recorded in my notebooks. The subject is not a simple one, as the diverse views of experienced astronomers on the similar problem of the motions of prominences indicate. Although the results given in the present paper are fragmentary, I hope they may serve in some measure to stimulate future work by observers adequately equipped for either visual or photographic studies.

An examination of the series of spectroheliograms reproduced in Plate IV will show that the most conspicuous phenomena here recorded by Ellerman are two dark ($H\alpha$) flocculi, rapidly changing in form as they are shot outward from a region, in some cases (espe-

[1] *Contributions from the Mount Wilson Observatory, Carnegie Institution of Washington*, No. 393.

[2] *Mt. Wilson Contr.*, No. 388; *Astrophysical Journal*, **70**, 265, 1929

cially at 6^h 39^m) appearing as a bright flocculus, on the preceding edge of a large sun-spot.

By way of contrast, another series of spectroheliograms, also taken on Mount Wilson in 1908, may be found in my first paper on "Solar Vortices."[1] A long dark hydrogen flocculus, which had been photographed on several days with comparatively little change of form, lying at a distance of about 150,000 km from a sun-spot, was suddenly drawn toward the spot at a velocity of the order of 100 km/sec. Four spectroheliograms were fortunately taken by St. John during the fifteen or twenty minutes while the rapid inflow was in progress. Such photographs, which are very rarely obtained, leave no doubt regarding the direction of flow or its approximate velocity. But, as my observations with the spectrohelioscope cited below illustrate, they fail to record some of the most important phases of such phenomena whenever the high radial velocities throw parts of the *Hα* line completely off the second slit of the spectroheliograph.

Spectroheliograms of prominences at the limb have been shown by Pettit to indicate accelerating inflow in most cases and outflow in others:

> Occasionally a streamer may be projected from one of the wings away from the spot, or a spike rise from the region of the spot. This is not the normal condition, however.[2]

Evershed, whose long experience with the solar spectroscope and spectroheliograph renders his conclusions of great value, gives a discussion of his work in the Kodaikanal *Memoirs*.[3] After stating that "all our experience at Kodaikanal goes to prove the essential identity of the filaments (long dark flocculi on the disc) and the prominences which have been photographed here" (p. 111), he gives many other conclusions, some of which will be referred to later. Among these one may be cited now: "The prevailing type of prom-

[1] *Mt. Wilson Contr.*, No. 26, Plates XXXVIII and XXXIX; *Astrophysical Journal*, **28**, 100, Plates XI and XII, 1908.

[2] "The Forms and Motions of the Solar Prominences," *Publications of the Yerkes Observatory*, **3**, Part IV, 232, 1925. See also Part I of the present article, *Mt. Wilson Contr.*, No. 388; *Astrophysical Journal*, **70**, 300, 1929.

[3] John Evershed and Mary Acworth Evershed, "Results of Prominence Observations," *Memoirs of the Kodaikanal Observatory*, **1**, Part II, 1917.

PLATE IV

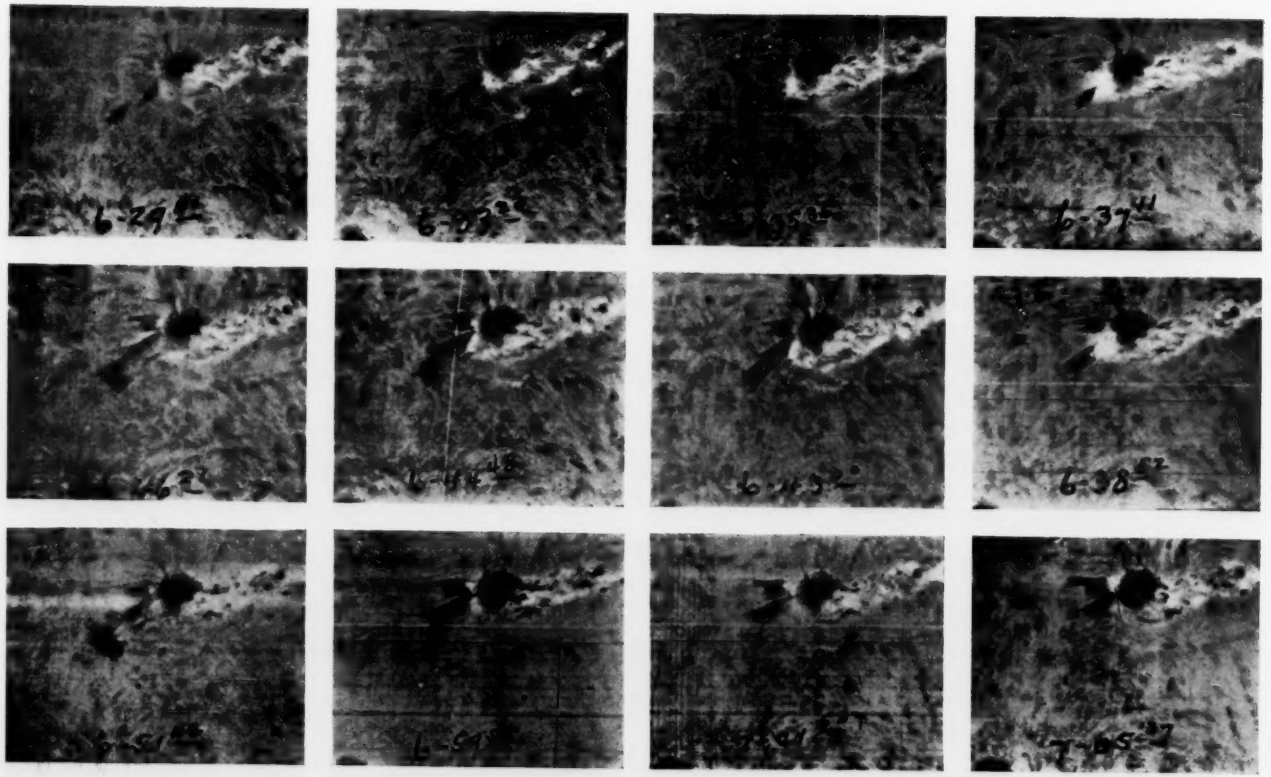

RAPIDLY CHANGING FLOCCULI NEAR LARGE SUN-SPOT, SEPTEMBER 10, 1908

inence found above sun-spots is the Rocket, called by Fényi 'Fleckenkrone,' which consists of jets and streamers radiating from the sun-spot."

In this type of prominence, as Fényi showed in 1892, the changes are rapid and the motion outward.

Evershed's general conclusion (p. 123) will also be of interest here: "Sixty thousand Kodaikanal prominences, and eleven thousand from Kenley, and other thousands from Rome, Sicily, Kalocsa, yet we cannot take one prominence and say: This caused it, thus and thus it began, and developed, and ended."

The fact is that the problem, both observational and theoretical, is complicated and important enough to call for the widespread application of any promising devices that may aid in its solution. The score of spectrohelioscopes already constructed or ordered, after the designs given in my last paper,[1] are especially adapted for this work, because they show many prominences on the disk and also at the limb, render visible masses of hydrogen moving at high speeds which are frequently not recorded by the spectroheliograph, and give an instant measure of the radial velocities of their various parts. It should be remembered, however, that the spectroheliograph is much better adapted for recording the forms of most of the flocculi, especially the fainter ones and those of minute and complex structure. The chief uses of the spectrohelioscope are the detection and study of intense and rapidly moving flocculi and the velocity analysis of prominences.

OBSERVATIONS WITH THE SPECTROHELIOSCOPE

The first satisfactory observations of hydrogen flocculi with a spectrohelioscope were made at my Solar Laboratory in Pasadena on January 16, 1924. On January 18 I tried moving the second slits across $H\alpha$ while observing (five slits were then used at each end of the oscillating bar, as described in the paper just cited), and found that the widely different forms of the flocculi corresponding to different wave-lengths could be beautifully seen in this way. On January 22, after further observations by this method, it became evident

[1] "The Spectrohelioscope and Its Work: Part I," *Mt. Wilson Contr.*, No. 388; *Astrophysical Journal*, **70**, 265, 1929.

that it would serve as a very quick and effective means of distinguishing between approaching and receding flocculi. On January 23 vortex phenomena in a spot group were clearly seen and partially analyzed. The next day the distortions of *Hα* near a brilliant eruption on the sun's disk were so pronounced that the forms of dark descending masses could be seen when the second slits were well beyond the extreme (red) boundary of the dark wings of *Hα*. On January 25 the eruption was very large and brilliant, and beyond it dark flocculi were descending at high velocities toward the largest spot in the accompanying group. The following day the large eruption had subsided, but a very small brilliant flocculus was seen at $12^h\ 10^m$ P.S.T. on the outer edge of the bridge separating the umbrae of the largest spot. This lasted only a few minutes, after which a long slender dark flocculus appeared, moving outward from the same point, evidently similar in type to the outflowing dark flocculi shown in Plate IV. Small short-lived bright flocculi also developed intermittently near this spot on January 27, where dark vortex structure could also be seen by setting the second slits at the wave-lengths corresponding to the radial velocities of the moving gases.

During this period, though the oscillating slits were still crude and my observations necessarily fragmentary, I could thus appreciate some of the possibilities of the spectrohelioscope, with which I also observed the tips of prominences moving rapidly toward spots at the sun's limb (as in the photographs reproduced by Slocum and Pettit), the remarkable effects of radial velocity in prominences projecting partly beyond the limb and partly (as dark flocculi) upon the disk, and the rapid flow (on Feb. 17) of such a flocculus toward a spot. Passing over some curious observations of radial motion and apparent absorption effects in prominences at the limb, of the appearance of spots in the light of the D lines, of bright eruptive regions observed with nicol and revolving half-wave plate, and of vortices associated with sun-spots, I come to an observation that bears directly upon the subject of this paper. My instrument, not yet completed, had been equipped with a pair of single oscillating slits and a plane-parallel glass plate below them (the "line-shifter" previously described) for setting any part of the *Hα* line or neighboring wave-

lengths on the oscillating second slit while the sun was under observation.

I referred in Part I of this paper to a typical dark arch seen on May 31, 1926, near the spot Mount Wilson No. 2571, then not far from the center of the sun. The appearance in the spectrohelioscope was approximately as shown in Figure 1, which is copied from a rough sketch in my notebook, made at $2^h\ 40^m$ P.S.T. The spot was at *A* and the small bright flocculus at *B*. The portion of the dark arch *C* was of maximum intensity when the second slit was off the *Hα* line to the violet. As *Hα* was moved across the slit with the line-shifter the following portion of the arch appeared. When the maximum of intensity in the arch reached *D*, the line was nearly central on the second slit. The rest of the arch did not appear until the red side of *Hα* was brought on to the slit. This terminated in a small black head at *E*, which was blackest when the second slit was well beyond the visible wing of the line to the red. This effect was repeatedly observed by turning the line-shifter, but at $2^h\ 55^m$ it was much less marked.

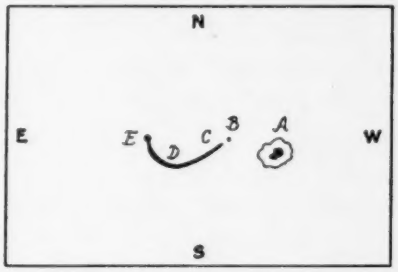

FIG. 1.—Arched flocculus observed on May 31, 1926, near the unipolar spot Mt. Wilson No. 2571.

The inference is plain. Hydrogen, rising from the bright flocculus at *B*, with a radial velocity sufficient to displace *Hα* well to the violet, followed a trajectory which was nearly at right angles to the line of sight at *D* and descended with high radial velocity at *E*. The termination of the arch in a small black head is an interesting phenomenon, frequently observed since that time, especially on the outer edge of the penumbra of spots, at the extremity of an inflowing flocculus.

Such an inflowing flocculus, typical in behavior and important in its bearing on the nature of the currents in the solar atmosphere, was seen in several of its phases on June 26, 1926. When observing at $4^h\ 45^m$ the preceding member of the large bipolar spot Mount Wilson No. 2598 (N 21°, E 26°, approx.), I noticed west of it a strong

dark flocculus which I had not seen at 3^h. The glass plate used for a line-shifter was a provisional one, and was not yet equipped with a divided circle. Thus I had to estimate displacements of the slit from the center of *Hα*, and as I was not then accustomed to the observation of rapidly changing flocculi, my record is imperfect. Nevertheless, it will serve to give an idea of what to look for in a case of this kind.

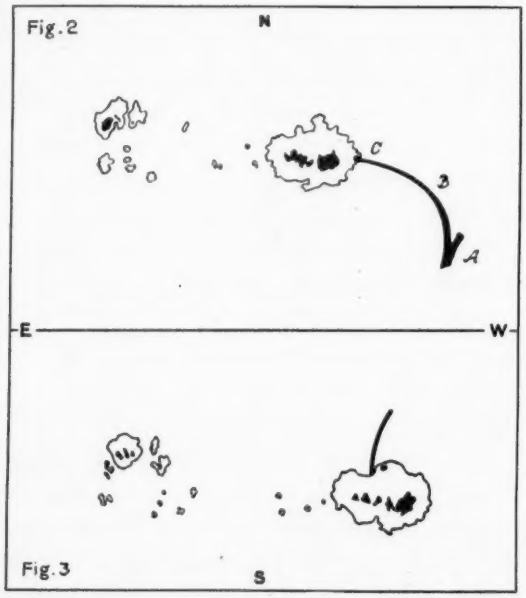

FIG. 2.—Flocculus observed on June 26, 1926, approaching preceding spot of large bipolar group Mt. Wilson No. 2598.

FIG. 3.—Flocculus observed on June 28, 1926, receding from preceding spot of bipolar group Mt. Wilson No. 2598.

At $4^h\ 52^m$, with a second slit half again as wide as *Hα*, the flocculus appeared nearly as in the composite sketch reproduced in Figure 2. The outer extremity was most intense when the center of the slit was more than an angstrom from the center of *Hα* toward the violet, and at this slit position the inner end of the flocculus did not reach the penumbra. When the center of the slit was nearly an angstrom to the red of *Hα* the appearance was similar, but the tip now touched the penumbra, though the small black dot noticed later at *C* was

not then seen. Puzzled at first by these phenomena, I soon recognized that the second slit was too wide, and closed it to about half its previous width, or about 0.8 the width of *Hα*. At 5^h 10^m, with the slit well beyond *Hα* to the violet, the flocculus had shortened, as though the outer hydrogen had flowed toward the spot. At 5^h 18^m the whole flocculus was faint with the slit central on *Hα*, and became very faint or disappeared at shorter wave-lengths. Three minutes later, with the slit about an angstrom toward the red of the center of *Hα*, nothing was observed but a small black dot at *C*, which fell exactly on the outer boundary of the spot's penumbra. After this time a portion of the curved flocculus could be faintly seen by moving toward *Hα* (slit overlapping its red edge). At 5^h 34^m the black dot on the penumbra appeared to be of maximum intensity at a slit position about half an angstrom to the red of *Hα*, and this was the condition at 6^h 10^m, when the rest of the flocculus had practically disappeared (for any slit position).

According to Rowland, the width of the normal dark *Hα* line is 0.963 A, or, including the extreme shading, 1.240 A. Judged from the width of the bright *Hα* at the base of the chromosphere, the shading is actually wider than this. Therefore, a dark hydrogen flocculus without motion in the line of sight may be visible when the second slit, even if extremely narrow, is anywhere within 0.5 or 0.6 A, or even more, from the center of the line.

The flocculus appears of greatest intensity when the slit coincides with the position of maximum absorption of the portion of the *Hα* line corresponding to the region in question. If, because of local radial velocity or other cause, this position of maximum absorption is shifted toward red or violet, the second slit must be displaced an equal amount in order to show such parts of the flocculus with maximum contrast. With a wide second slit (on the assumption that the flocculus is exceptionally intense), even those parts moving toward or away from the observer at considerable velocity may be visible at the same time.

With these points in mind it is easy to include the foregoing observations in a single progressive picture. At some time after 3^h an intensely dark flocculus was shot upward near the point *A*. At 4^h 45^m it was still rising rapidly, but the absorbing gas had been drawn

toward the spot and its narrowed tip was already descending toward the outer edge of the penumbra. At $5^h\ 10^m$ the dark mass at *A* had disappeared and the maximum of intensity had moved about halfway toward the spot to *B*. The outer part of the flocculus continued to fade and by $5^h\ 21^m$ the maximum of intensity had shifted to the round black dot at *C*, moving downward with a radial component of some 60 km/sec. At $6^h\ 10^m$ the dot on the penumbra was still black, though apparently descending less rapidly, and the rest of the flocculus had almost completely faded away.

This observation, which recalls the almost unique spectroheliographic results of June 3, 1908, was followed on June 28 by an eruptive outflow from a different part of the same (preceding) spot of the bipolar group. A small bright region appears at the north side of the penumbra of this spot on a direct photograph taken by Ellerman with the 60-foot tower telescope the same morning (June 28, about 6^h). At $10^h\ 09^m$, I saw with my spectrohelioscope in Pasadena a bright flocculus at this point, when the inner edge of the second slit was just touching the violet edge of *Hα*. Eight minutes later a narrow dark flocculus, nearly straight, extended from the same point to a distance about equal to the width of the penumbra of the large spot (Fig. 3). At $10^h\ 20^m$ only the outer extremity of the flocculus could be seen with the second slit in the same position as in the two previous observations. When the slit was moved farther toward the violet, the maximum of intensity advanced along the dark flocculus toward the spot, ending at the edge of the penumbra. Intermittent renewals of this outflow, bright and dark, appeared later in the day. The hydrogen, rising at intervals from the bright point near the end of the bridge, traveled outward toward the north, reaching its maximum distance at about $3^h\ 30^m$, at a point where a short, somewhat elongated dark flocculus was seen descending with a radial component of about +60 km/sec.

Omitting various observations of outflow and inflow, made during a period chiefly devoted to experiments with various forms of spectrohelioscopes, we come to some results obtained on August 15, 1926, when improved optical and mechanical parts had been installed and the parallel-plate line-shifter provided with a divided circle for radial-velocity measures. In the first part of this paper

one of these inflowing flocculi (here shown as Fig. 4, *GHI*) was illustrated to explain the method of observation, but the others also deserve mention.[1]

The first inflow (Fig. 4, *ABC*) was seen at $10^h\ 15^m$, rising at some distance from the following spot of the pair (Mt. W. No. 2656) and terminating in a small black head descending with moderate velocity toward the outer edge of the penumbra. At $10^h\ 22^m$ another curved

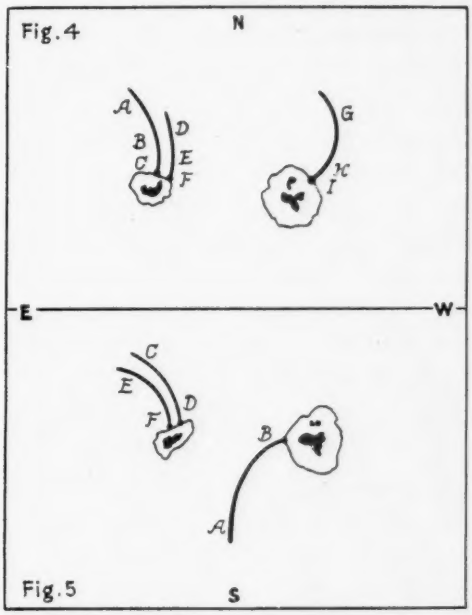

FIGS. 4, 5.—Flocculi observed on August 15 and 16, respectively, approaching both spots of the bipolar group Mt. Wilson No. 2656.

flocculus (Fig. 4, *DEF*) was sketched near the first one. The effect was precisely similar, except that the final black head was descending with higher velocity in this case, and could be seen alone on the edge of the penumbra, when the second slit was well beyond the normal *Hα* line toward the red, at a wave-length where the whole of the first flocculus had disappeared. In both cases, as the line-shifter was rotated, the outer ends of the curved flocculi appeared when the second slit was on the violet side of *Hα* and the maximum

[1] *Ibid.*

of intensity moved steadily along them as the wave-length of the light entering the second slit increased. I was so absorbed in the observations that I forgot to determine the slit zero, and therefore cannot give the radial velocities, though my sketches corresponding to four different line-shifter records show the effects described. At $10^h\ 44^m$ the first flocculus had nearly faded out and *DEF* was weak. At $10^h\ 51^m$ traces of the extremities of both flocculi close to the spot could be seen on the red side of *Hα*, but neither flocculus was visible with the second slit on the center of the line.

A still finer effect of inflow, first observed near the preceding spot at $10^h\ 57^m$, which was described (with its radial velocities) in my last paper, is also shown here in Figure 4 (*GHI*).

On the following day a beautiful case of the same kind was observed at $10^h\ 0^m$. A long curved flocculus (Fig. 5, *AB*), originating in a bright eruptive region south following the preceding spot of the same group, terminated in a black head exactly on the following edge of the penumbra, where its radial velocity approached +30 km/sec. A nearly parallel flocculus (not shown in Fig. 5) gave the same effect, which was also given to even better advantage by two parallel curved flocculi (*CD* and *EF*) seen descending toward the following spot at $10^h\ 25^m$. All of these showed the same characteristic appearance, again confirmed on August 17: the apparent advance toward the spot of the inner extremity of the flocculus as the line-shifter was turned so as to bring light of greater wave-length upon the oscillating second slit.

As already remarked, a notable fact, true for all these cases of inflow and for many others since observed, is the termination of each flocculus in a definite black head, usually nearly circular when observed alone well to the red of *Hα*, but sometimes accompanied (at the slit position giving maximum intensity) by a short tail. In many instances this head falls precisely above the outer edge of the penumbra of the spot, which is perfectly visible when the second slit is beyond the wings of *Hα*. This head, the advance of the maximum of intensity, and the considerable velocity of descent are the most striking features of such phenomena.

On September 11, 1926, having returned to Pasadena after an absence of several weeks, I again confirmed the foregoing effects.

In some instances, as illustrated below, the tip of the inflowing flocculus undoubtedly reaches a point above the edge of the umbra of the spot; but when the second slit is so placed in wave-length as to show the head at its blackest, its center will often be found to lie above the narrow outer boundary of the penumbra. As the seeing in Pasadena is rarely or never good enough to permit the use of high magnifying powers in solar observations, I hope this phenomenon will ultimately be studied minutely elsewhere under more perfect atmospheric conditions.

On September 13 two interesting cases of inflow were observed in conjunction with the spots of a bipolar group, the following member of which was very close to the east limb. A small, curved, dark flocculus was first noticed at $10^h\ 15^m$ just behind the following spot, extending from it to the limb. It could not be seen at circle readings from +10 (red) to −15 (violet), but first appeared at −15 as a dot almost touching the limb. As the line-shifter was turned farther toward the violet a curved extension from this dot approached the spot, appearing as a point on the penumbra when the circle indicated a (tangential) velocity of approach of some 50 km/sec. At $11^h\ 30^m$, just behind the preceding spot of the pair, a flocculus, appearing bright on the disk and extending beyond the limb as a curved prominence, was also seen to be approaching the spot.

I reserve for another section of this paper a discussion of hydrogen vortices in the solar atmosphere, which are usually best studied in their simplest form, associated with single spots.[1] The hydrogen arches and inflows accompanying active bipolar groups, however, often present very striking phenomena, some of which will be described here.

The great bipolar spot group Mount Wilson No. 2686, at about 24° north latitude, was well advanced on the sun's disk when examined with the spectrohelioscope on September 16, 1926. The accompanying outline of the spots was traced from the polarity record made by Nicholson with the 150-foot tower telescope on Mount Wilson at $9^h\ 10^m$, and some of my own later observations of inflowing flocculi have been sketched in at their different positions (Fig. 6).

[1] For a preliminary discussion see "The Fields of Force in the Atmosphere of the Sun," *Nature*, **119**, 708, 1927.

At $12^h\ 15^m$ I observed a clearly defined (dark) hydrogen inflow *AB*, which seemed to reach the central umbra of the following spot. Before I could complete a satisfactory set of measures my attention was attracted by a forked flocculus *CD* reaching the preceding umbra in this spot, which it certainly seemed to touch at $12^h\ 32^m$, when its inner end showed a marked radial velocity of recession. The

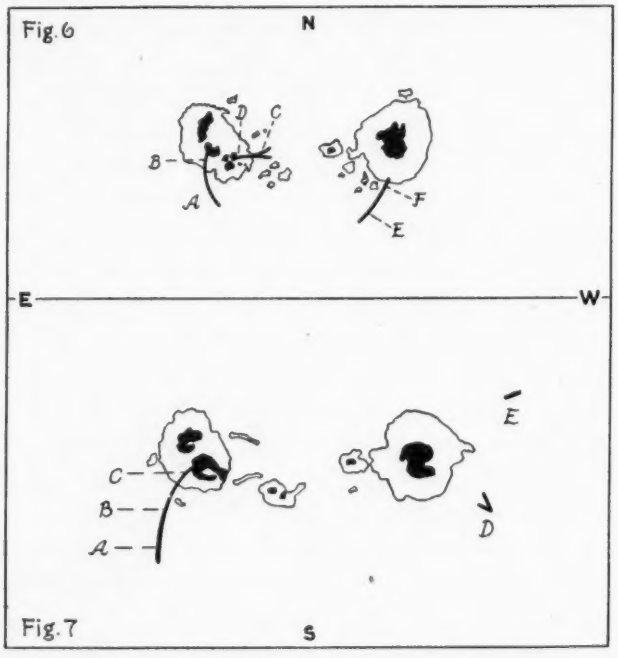

FIG. 6.—Flocculi observed on September 16, 1926, approaching both spots of the large bipolar group Mt. Wilson No. 2686.

FIG. 7.—Flocculi observed on September 17, 1926, near bipolar spot group Mt. Wilson No. 2686.

outer forked end *C*, the southern branch of which was darker than the northern, appeared to be nearly stationary in the line of sight. At $2^h\ 36^m$ another fainter inflow, which also seemed to reach the umbra, occurred near the same point. Several active bright flocculi appeared at various times during the day between the preceding and following spots of the bipolar group, two of which were very bright at $2^h\ 58^m$, when they gave a width of 1.8 A for *Hα*.

At 2^h a dark linear inflowing flocculus *EF* was seen south of the preceding spot. Its outer part *E* was seen alone on the violet side of *Hα*. Nearer the spot the radial component reached zero and attained a positive value of some 30 km/sec. in the black, slightly elongated head *F*, which centered exactly upon the outer boundary of the penumbra. This was apparently a case of an arch, composed of absorbing hydrogen, which rose south of the spot and descended toward the penumbra. Later in the afternoon the active bright flocculi fluctuated in intensity, but had disappeared at 5^h. A dark linear arc was then seen, rising near the east boundary of the large preceding spot and descending toward the west umbra of the following spot, but the sun was too low for satisfactory measurements.

On September 17 the same spot group showed some additional cases of inflow, two of which are sketched in Figure 7 on a tracing of the polarity drawing made on Mount Wilson at $8^h\ 30^m$ that morning by Pettit. At $11^h\ 05^m$ a very dark linear flocculus, which had not been noticed before, was suddenly seen as a short black line at *A*, with a radial velocity of about -20 km/sec. As the wave-length of the transmitted light was increased by the line-shifter, the flocculus was seen to lengthen toward the spot, though its maximum intensity just outside the penumbra could not be well determined because of a bright flocculus there. A series of measurements was made at six points along the flocculus, however, showing velocities changing from approach to recession, and indicating a faint extension to the central umbra of the following spot at $11^h\ 28^m$. Two minutes later I found that changes of intensity (for the same wave-length) had occurred near the point *B*, where the radial component was about +40 km/sec. At $11^h\ 35^m$ the tip was noted as apparently reaching the umbra, with a higher velocity of recession. One minute later nothing but a short length at the inner extremity *C* could be seen with the second slit well to the red of *Hα*. Another similar inflow, along a closely adjacent path, from a point somewhat farther from the spot, was observed about fifteen minutes later. The values of the radial velocities are uncertain, because the slit zero did not at that time always remain constant, owing to some instability in the parts of the spectrohelioscope. No very bright flocculi were then seen in or near the group. At $2^h\ 32^m$ two short dark flocculi (Fig. 7,

D and *E*), both rising rapidly, were seen west of the preceding spot. I was called away at that time, and could do no more than to note the fact of their ascent and also that one of them was forked, as indicated roughly in the sketch at *D*, where their positions are only approximate.

On September 18 I observed some of the phases of a striking phenomenon, repeatedly seen in slightly varying form on several successive days. After noting an apparent case of inflow near the preceding spot of the bipolar group, I saw at $11^h\ 56^m$ a very strong black flocculus *A* with a velocity of approach of about -40 km/sec., which had appeared very suddenly. It showed the beginnings of a forked structure, more fully developed four minutes later, when the general appearance of the flocculus was as shown in Figure 8, at a setting of the line-shifter corresponding to -30 km/sec. The faint curved arc, apparently extending from the point of the fork to the western extremity of the umbra of the following spot, was not seen in the first observation. At $12^h\ 03^m$, at the same wave-length, the flocculus was noted to be fading. At $12^h\ 12^m$ the fork, at a setting corresponding to $+16$ km/sec., no longer retained its form or position, but seemed to have split into two faint arcs, with an open space between them, moving in opposite directions toward the preceding and following spots (not shown in the figure, but at the approximate positions *B* and *C*). At $12^h\ 21^m$ nothing was seen (at any wave-length) excepting the two inflowing flocculi shown at *D* near the following spot in Figure 9 (radial component about $+20$ km/sec.). At $12^h\ 25^m$ these were fainter and had apparently reached a point above the western tip of the umbra (Fig. 9, *E*, radial component about $+26$ km/sec.). A minute later these flocculi at *E* had disappeared, but another single curved dark flocculus, with a radial component indicating ascent, had arisen at about the position *D*.

Even with the spectrohelioscope, constantly aided by the line-shifter, it is difficult to follow these varying phenomena. Their quick changes in position and wave-length, and the recurrence of new flocculi, rapidly ascending at nearly the same points, show what difficulty there would be in photographing and analyzing them satisfactorily with a spectroheliograph, even with visual guidance by an observer at the spectrohelioscope. As the scale of the photographed

image should be large enough to show sharply the slender details of the flocculi, and repeated exposures (necessarily rather long with most existing instruments) must be made at different settings of *Hα* on the second slit, the tasks of photography and measurement

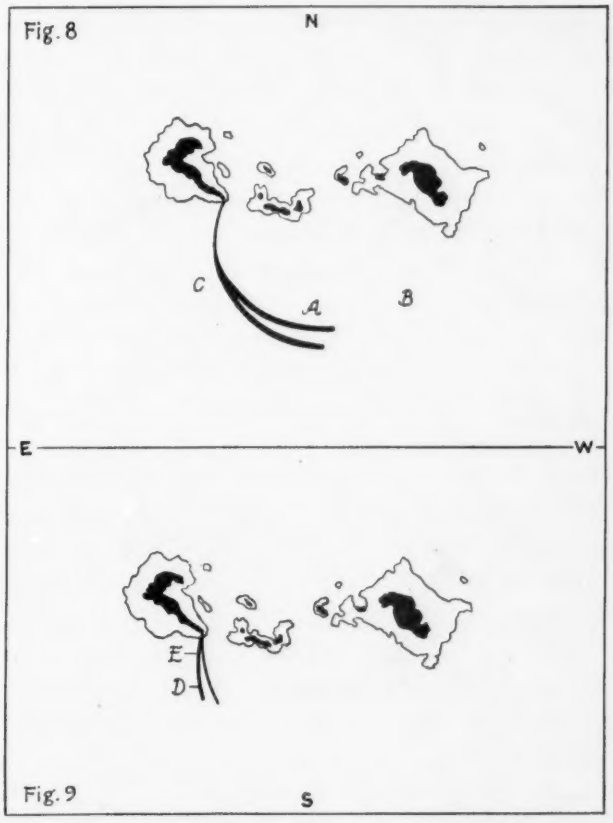

FIGS. 8, 9.—Flocculi observed on September 18, 1926, near bipolar spot group Mt. Wilson No. 2686.

are not easy.[1] On the other hand, it is very difficult with the spectrohelioscope alone to make accurate records of what one readily sees. All of the drawings reproduced in this paper are rough and

[1] I think that an optical combination of comparatively large angular aperture, such as the 40-inch Yerkes refractor and the Rumford spectroheliograph, could be adapted for making good photographic records of the phases of phenomena like those shown in Figs. 8 and 9.

schematic, but they will at least serve to indicate the general character of the phenomena. It is of course to be understood in every case that only a few flocculi of special interest have been picked out for record, though many others were seen; we must turn to the

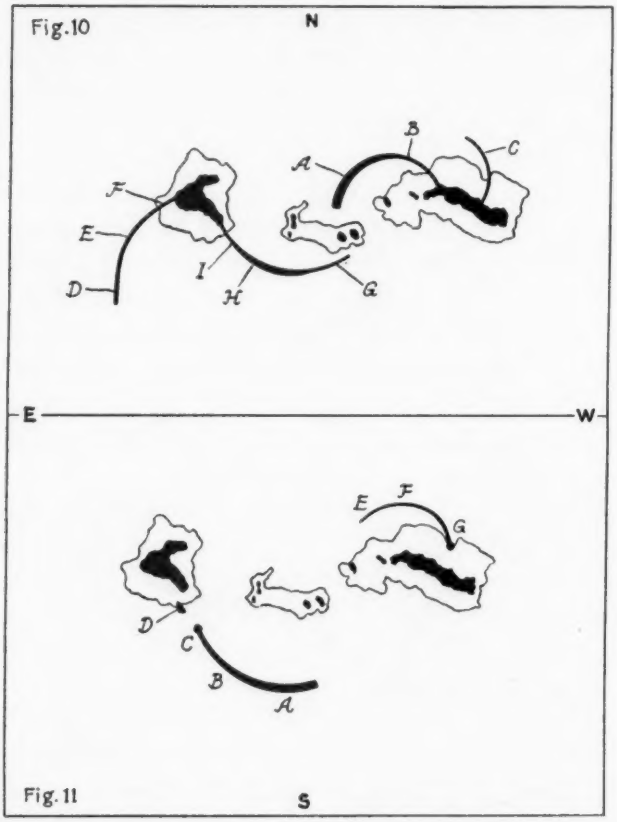

FIGS. 10, 11.—Flocculi observed on September 19, 1926, near bipolar spot group Mt. Wilson No. 2686.

spectroheliograph for the best means of showing the complex structure of the flocculi always present on the sun.

On September 19 the large bipolar group, as shown by Pettit's polarity sketch at $10^h\ 45^m$, was crossing the central meridian of the sun (Figs. 10 and 11). Soon after ten o'clock I saw at Pasadena with the spectrohelioscope a strongly marked dark flocculus, not

very intense at its inner end, which reached the umbra of the preceding spot (*B*, Fig. 10, radial component from +80 to +100 km/sec.), but broader and very black at its point of maximum intensity (*A*, Fig. 10, radial component +60 km/sec. at $10^h\ 12^m$). A nearly parallel faint slender curved flocculus was seen at $10^h\ 15^m$ near *A*, at a slit position corresponding to a radial component of about +40 km/sec., where the first flocculus at *A* was much fainter. At about the middle of *Hα* both of the parallel flocculi extended farther south than I is carried in the sketch. At $10^h\ 26^m$, and again four minutes later, I repeated the observation of the inner tip touching the umbra, and found it very short (reaching only to about *B*) and more intense than at first, with a radial component of about +110 km/sec. The line-shifter was then turned back and forth, permitting the whole length of the flocculus (*A* to umbra) to be repeatedly observed. At $10^h\ 38^m$ it had almost completely disappeared (for any wave-length), though the inner end could be faintly seen, still rapidly descending. Both of the oscillating slits, it may be added, were 0.003 inch wide, less than half the width of the normal dark *Hα* line.

Another faint curved inflow *C*, also descending rapidly and reaching the long umbra of the preceding spot farther to the east, was suspected at $10^h\ 26^m$ and definitely confirmed at $11^h\ 03^m$.

I then turned my attention to the following spot and saw another fine inflow at $11^h\ 12^m$. The maxima of intensity at different parts of the arc corresponded to the following approximate radial components: *D*, +14; *E*, +32; *F*, +54 km/sec. The inner end, which appeared to reach the umbra, was darker than that of the flocculus *AB*. Another inflow *GHI*, showing a greater range of velocity, was noticed at $11^h\ 24^m$, with the following approximate radial components: *G*, +8; *H* (very dark), +26; *I*, +86; tip touching umbra, +114 km/sec. The last measurement was made at $11^h\ 30^m$. Ten minutes later the descending tip at the umbra had about the same radial velocity, but was fainter.

Another inflowing flocculus, which suddenly developed about $11^h\ 50^m$, is shown in a separate sketch (Fig. 11, *AC*), to avoid confusion. At $11^h\ 57^m$ it appeared approximately as from *A* to *B* (very black, radial component about +12 km/sec.) but the black head *C* showed

with maximum intensity at +36 km/sec. Four minutes later the black head was seen as a short line *D* on the edge of the penumbra (radial component about +50 km/sec.). In this position of the second slit the outer part *A* could also be seen (indicating a greatly widened *Hα* line at this point), but the intermediate region *B* was invisible. At $12^h\ 01^m$, at a wave-length corresponding to a radial component of +74 km/sec., nothing was visible but a very black dot on the edge of the penumbra. Another very black curved flocculus, seen at $4^h\ 15^m$, flowed toward the following spot, but it faded so rapidly that satisfactory measures could not be made. At one position of the second slit the inner end seemed to reach the umbra, but farther toward the red (radial component about +52 km/sec.) it was seen to terminate as a dot (now fainter) on the edge of the penumbra. At $4^h\ 53^m$ another dot (inflow), with about the same radial velocity, was observed at the same point.

The last inflow seen on September 19 is shown at *EFG*. The outer part *E* was darkest, with a radial component of about −32 km/sec., but farther toward the red (−8 km/sec.), the arc advanced toward the penumbra. Still farther (about +34 km/sec.), nothing remained but the very black point *G*, descending toward the edge of the penumbra.

On September 20 the seeing was better than usual in Pasadena. A well-defined inflowing flocculus *ABC*, sketched in Figure 12 on a tracing of the polarity drawing made by Pettit at $11^h\ 15^m$ the same day on Mount Wilson, was observed at $9^h\ 10^m$ with the spectrohelioscope. Its inner end met the umbra exactly at the end of a narrow bridge recorded in my notes as extending across the umbra (when seen with the light of the continuous spectrum far from *Hα*), but not shown in Pettit's later direct image. The tip *C* was descending at $9^h\ 23^m$ toward the umbra with a radial component of about +60 km/sec. Near the center of *Hα* the tip could not be seen, but the part of the arc at *B* (not visible at the previous wave-length) was observed alone. Farther toward the violet were the fainter ascending parallel arcs indicated at *A*, which very likely had previously been more intense, if we may judge from earlier observations of this character. At $10^h\ 13^m$, and also at $12^h\ 08^m$, the tip *C* was visible, again noted as meeting the end of the bridge across the umbra and

as very black across the penumbra when the line-shifter indicated a radial component of between +40 and +50 km/sec. At $12^h\ 13^m$ two cases of inflow, having a smaller radial component of recession

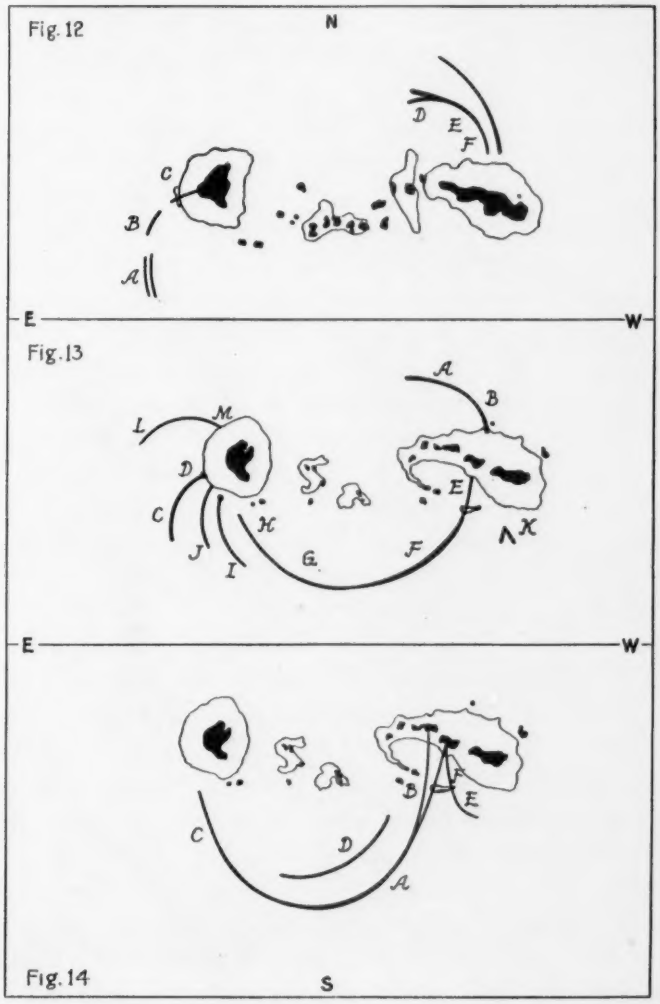

FIG. 12.—Flocculi observed on September 20, 1926, near bipolar spot group Mt. Wilson No. 2686.

FIGS. 13, 14.—Flocculi observed on September 21, 1926, near bipolar spot group Mt. Wilson No. 2686.

at the inner end, were seen reaching the preceding umbra on its north side, near the middle of its length.

In the afternoon, when the seeing was again recorded as exceptionally good, the fine structure of the field of force shown by the less intense flocculi on a spectroheliogram taken at $8^h\ 45^m$ that morning at Mount Wilson was plainly visible, approximately as in Plate V. The curvature of these flocculi on the south side of the preceding spot was noted to be as in the photograph, but no inflow (displacement of the maximum of intensity) could be detected along them with the line-shifter, though definite inflow of the opposite direction of whirl was seen on the north side of the umbra. Two brilliant small flocculi, first detected by my assistant, Mr. Hitchcock, about $12^h\ 30^m$, were recorded at $2^h\ 46^m$ on the penumbra of the preceding spot, a short distance northwest of the western end of the umbra. The width of the bright *Hα* line at these two points was then nearly 1.4 A, or about twice the normal for ordinary bright flocculi. But these bright flocculi, as is so often true, indicated little or no radial motion. At $3^h\ 41^m$ they were decidedly fainter, with a bright *Hα* line about 1 A wide.

At $3^h\ 50^m$, two inflowing curved flocculi were seen north following the preceding spot (Fig. 12, *DEF*). My rough sketch shows them approximately as they appeared five minutes later, when the line-shifter indicated a radial component of about +30 km/sec. At this setting the lower (southern) flocculus was more intense than the northern and forked at the outer end. The northern flocculus, faint at this time at its outer end, was visible alone at about the same setting at $4^h\ 10^m$, when the outer end had become stronger and the southern flocculus had disappeared. When first seen both flocculi extended farther southeast in longer arcs (as observed at the center of *Hα* and to the violet), curving down to reach a line prolonging the preceding umbra to the east.

At $3^h\ 28^m$, and again at 4^h, nearly linear dark flocculi, of a type (to be described later) which appears strong on both sides of *Hα*, were seen for short periods southwest of the large preceding umbra.

On September 21, as Nicholson's polarity drawing of the spot group made at $12^h\ 35^m$ shows (Fig. 13), the preceding umbra had divided into several parts. It is interesting to note, though perhaps

PLATE V

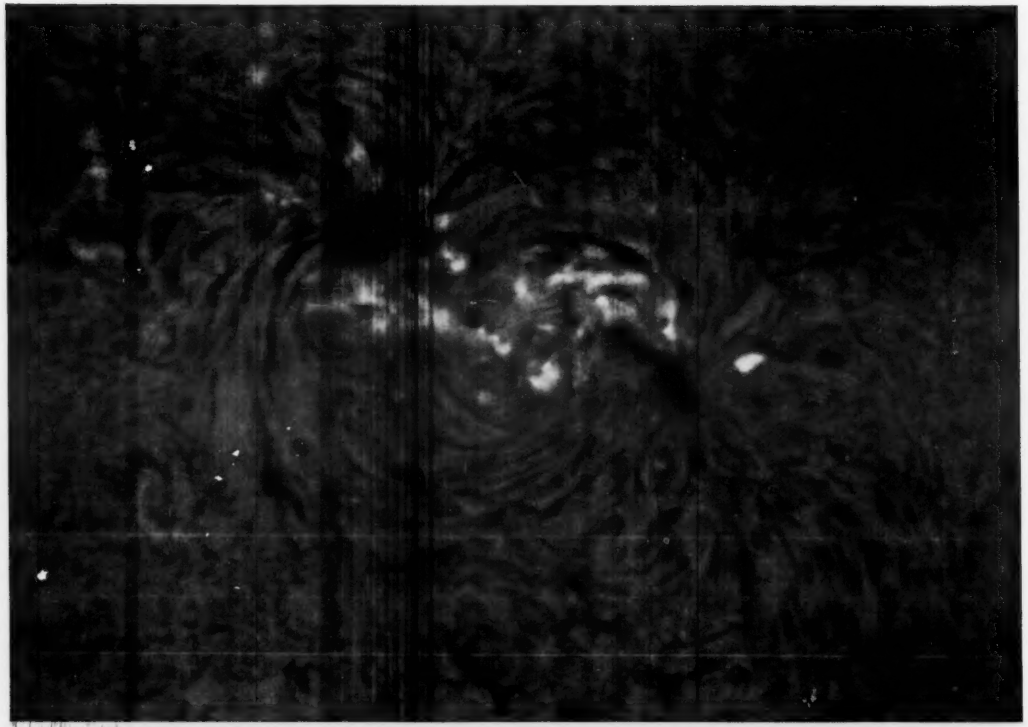

UNIV. OF MICH.

BRIGHT AND DARK HYDROGEN ($H\alpha$) FLOCCULI ASSOCIATED WITH THE BIPOLAR SUN-SPOT MT. WILSON NO. 2686

Photographed on September 20, 1926, $8^h\ 45^m$, by Edison Pettit with the 60-Foot Tower Telescope and 13-Foot Spectroheliograph.

merely as a coincidence, that two very small spots had appeared on or near its north penumbra, close to the terminations of the dark descending flocculi *FED* in Figure 12. At 9^h I noticed an inflowing curved flocculus (Fig. 13, *AB*), the head of which reached the penumbra, apparently at one of these small spots, with a radial component of about +28 km/sec. Its outer half *A* was seen alone, of maximum intensity at the center of *Hα*, where the inner part *B* was invisible. At 9^h 16^m another inflow (Fig. 13, *CD*) was seen terminating in a black dot (radial component about +34 km/sec.) on the outer edge of the penumbra of the following spot, near the position of the inflowing flocculus seen on September 20 (Fig. 12, *ABC*). Its outer part *C* was of maximum intensity at about −16 km/sec.

A curved dark flocculus (Fig. 13, *EF*), extending from the south and east toward the central umbra of the preceding spot, was observed at 9^h 54^m, but no satisfactory measurements could be made because my instruments were set into vibration by a tractor in motion not far from the Solar Laboratory. The inner end, though faint, seemed to touch the spot when observed at 10^h. Ten minutes later rapid changes of intensity were noted, the part near *F* appearing very dark on the violet side of *Hα*. At 10^h 31^m only the broader and rather fainter section of the arc at *G* was seen (radial component roughly −12 km/sec.). At 11^h 13^m the arc, as observed at the center of *Hα*, included *G* and a narrower extension toward *H*. At 11^h 21^m (radial component about +8 km/sec.), three or four curved dark flocculi (*H*, *I*, *J*), two of which showed definite inflow, were observed south of the following spot; the maximum of *I* moved toward the penumbra, though it did not reach it (11^h 24^m), when the line-shifter was turned, while the tip of *J* did reach the penumbra when the circle indicated a radial component of +38 km/sec. Seven minutes later *I* terminated in a black dot just outside of the penumbra, of maximum intensity at +18 km/sec.

It should be added that a small brilliant point flocculus (bright *Hα* about 1.5 A wide) was observed at 10^h 36^m. When examined on the violet side of *Hα* it was seen to be accompanied by two dark wings, which diverged from it, as indicated at *K*.

At 4^h 09^m another curved flocculus *LM* was seen approaching the large following spot of the pair. Its inner extremity *M* appeared

alone as a short, narrow, black line, crossed centrally by the outer edge of the penumbra, with a radial component of about +27 km/sec., while its outer part *L* was visible without this tip, when the second slit was nearly central on *Hα*.

Another sketch (Fig. 14) is needed to show the phenomena noted soon afterward. At $4^h\ 23^m$, on the red edge of *Hα*, the slender dark flocculus *AB* was seen, forked as indicated, the branches extending to the two principal following umbrae of the large preceding spot. Eight minutes later, at a setting near the center of *Hα*, the entire arc *BAC* was visible, accompanied by a shorter arc *D*. I was unable to make a satisfactory set of measurements, especially as some small bright flocculi appeared within a few minutes south of the preceding spot, about on the line of the western branch of the dark fork. At $4^h\ 49^m$ a dark flocculus *EF* was found to extend from these bright flocculi to the third umbra in the preceding spot. There were definite signs of inflow, and I was struck by the fact that the direction of the curvature was opposite to that of the arc *AB*. The seeing was excellent, and there seemed to be no doubt about the reality of these phenomena.

On September 22 the spot group, as shown by Ellerman's polarity sketch made on Mount Wilson at $6^h\ 45^m$, appeared as in Figure 15. At $9^h\ 02^m$ I saw in Pasadena the curved dark flocculus *ABC*, with a maximum radial component of about +38 km/sec. at the point *C* on the edge of the penumbra. As the line-shifter was rotated toward the violet the curve lengthened toward *B*, so that the arc *BC* was seen at about +20 km/sec. Farther to the violet the head *C* disappeared and the arc lengthened to *A*. It was seen at nearly its full length, though not quite reaching the penumbra, at about −6 km/sec. This was at $9^h\ 12^m$. At $9^h\ 45^m$ the inner extremity, from about *B* to *C*, was seen near the center of *Hα* to be split from *B* to *C* into a fork (similar to that shown in Fig. 14). The arms of the fork were faint but unmistakable at −12 km/sec., but were stronger at +20 km/sec. At $9^h\ 48^m$ both branches terminated on the penumbra at a setting corresponding to a radial component of about +48 km/sec. The preceding branch was very faint, without head, while the stronger following branch ended in a definite pointlike head, precisely on the outer rim of the penumbra.

PLATE VI

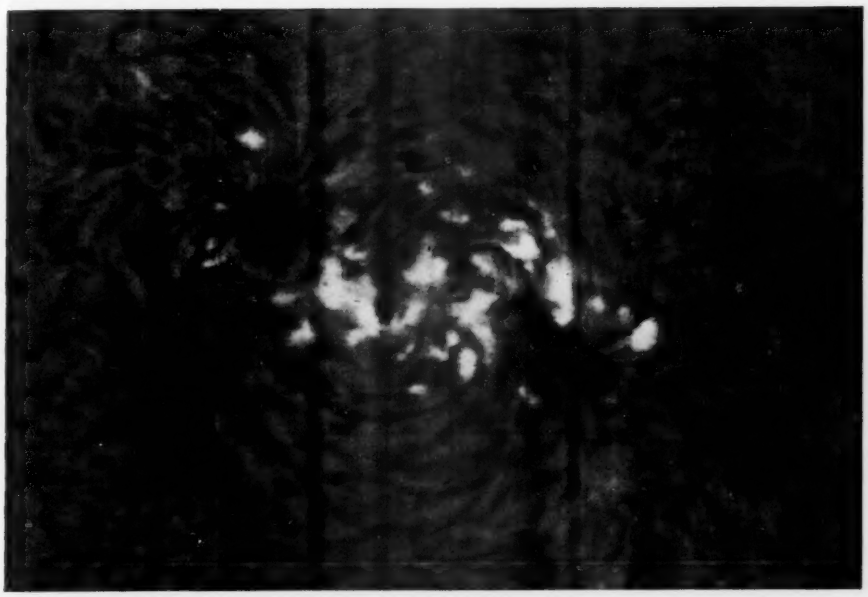

September 21, 1926, $6^h\ 40^m$

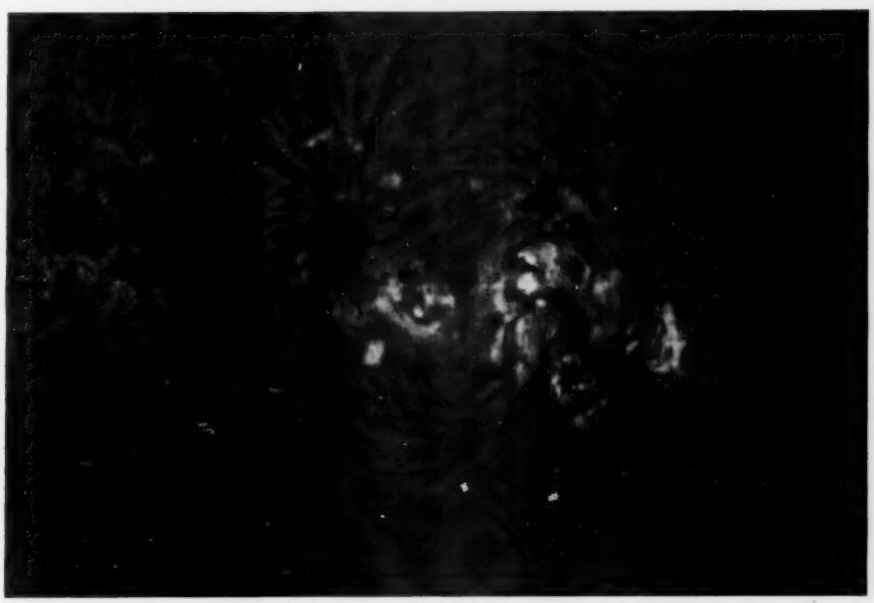

September 22, 1926, $6^h\ 49^m$

UNIV. OF MICH.

BRIGHT AND DARK HYDROGEN ($H\alpha$) FLOCCULI ASSOCIATED WITH THE BIPOLAR SUN-SPOT MT. WILSON NO. 2686

Photographed by Lewis Humason with the 60-Foot Tower Telescope and 13-Foot Spectroheliograph.

At this time the seeing was excellent, and the complex structure of the field of force in the flocculi surrounding the group could be

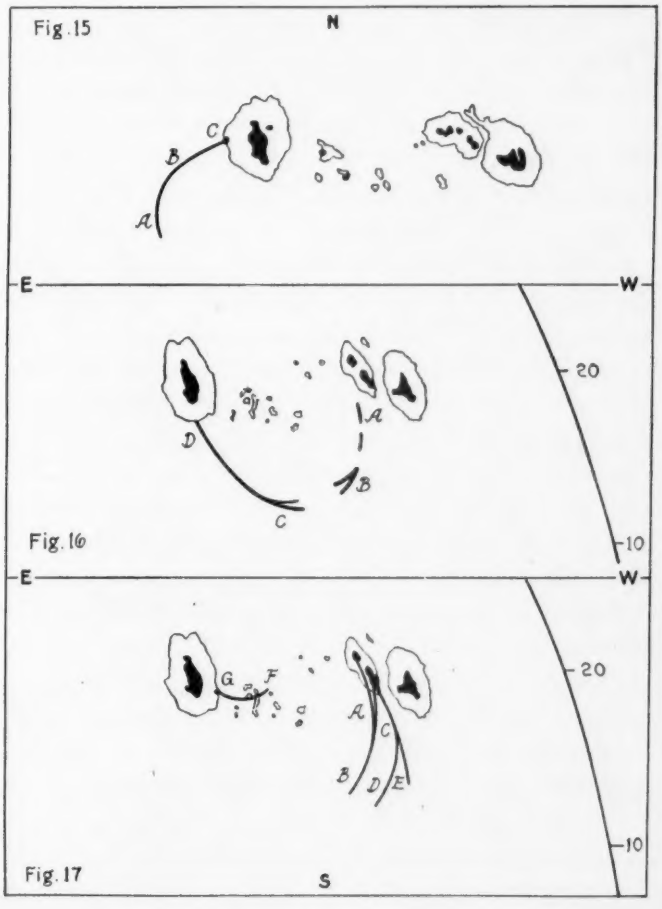

FIG. 15.—Flocculus observed on September 22, 1926, near bipolar spot group Mt. Wilson No. 2686.

FIGS. 16, 17.—Flocculi observed on September 23, 1926, near bipolar spot group Mt. Wilson No. 2686.

seen nearly as well as on the best spectroheliograms. North and south of the following spot the apparently inflowing slender flocculi appeared to be curved in opposite directions (clockwise and counter-

clockwise), a fact to be noted in my future discussion of the fields of force.

Passing over some other observations, to be mentioned later, we come to the phenomena seen on September 23. The preceding spot was 60° W. and the following spot 41° W. of the central meridian when Ellerman's polarity sketch was made on Mount Wilson at 6^h 36^m. At 10^h 12^m, after recording three fine cases of inflow on the south side of the preceding spots, I saw a long curved flocculus almost reaching the western member of the preceding pair and extending nearly to the following spot of the bipolar group (Fig. 16). The circle reading of the line-shifter was -15 (corresponding to a radial component of about -30 km/sec.), and when this was changed to -20, the maximum of intensity moved out along the arc from *A* toward *B*. At 10^h 38^m two forks not seen before had developed at *B* and *C*, one of which (*B*) was very black with the line-shifter at -23; at this setting only the arc from *B* to *D* was recorded. The forks weakened toward the red and were hardly visible beyond $+10$. My attention was diverted for a few minutes by another very black flocculus, first noticed at 10^h 31^m north of the following spot at a circle reading of $+13$, which seemed to originate in a bright flocculus and rapidly extended outward in two branches toward the north. At 10^h 47^m the crown of the arc *BC*, no longer forked, was very intense at -31, but invisible toward the red beyond the center of *Hα*. The rest of the arc (*CD*) was faint. At 10^h 56^m the crown of the arc appeared at -15 in two overlapping parts, not forked, the inner one now fading (though somewhat more intense at -19), while the outer arc extended to the western spot of the preceding pair, but disappeared east of *C*. At 11^h 20^m an arc of the opposite curvature (not shown in Fig. 16) was seen extending from a point near the center of the bipolar group toward the north following side of the western spot of the preceding pair.

Another cut (Fig. 17) is needed to show clearly my later observations on the same day. At 12^h 05^m, with the second slit nearly central on *Hα*, the three arcs *AB*, *CD*, and *CE* were seen. *AB* was split into a fork, the two branches of which appeared to reach the two umbrae of the western spot of the preceding pair. *DC* and *EC* united at *C*, from which point they continued as a slender dark line

to the nearer of these umbrae. Two minutes later, at a circle reading of −19, the fork (from A to the umbrae) was invisible, and the maximum of intensity of the arc was at *B*. The arc extending from *E* through *C* to the other umbra persisted faintly, but the arc *CD* was not seen.

In the afternoon, at $3^h\ 16^m$, the arc *FG* was observed. The outer extremity *F* was seen alone near the center of *Hα*. At a circle reading of −6 only the crown of the arc, curving about a small sun-spot, was visible. At $3^h\ 19^m$, when the line-shifter was set at −26, no trace of the arc could be seen excepting the black dot at *G* on the edge of the penumbra of the large following spot.

The arcs south of the bipolar group were renewed on September 24, and on the following day, when the preceding spot had almost reached the west limb, several slender prominences were seen projecting to heights of from 30,000 to 40,000 km. The first of these, observed at $10^h\ 30^m$ with first and second slits 0.006 and 0.004 inch in width, respectively, is shown in Figure 18. It had disappeared within a few minutes, before satisfactory measurements could be completed. At $10^h\ 58^m$ this prominence reappeared at about the same position, somewhat higher and brighter than before. With the comparatively wide slits employed its entire length was visible near the center of *Hα*, but the line-shifter showed that the maximum of intensity of its upper part was to the violet of that at the base, implying for its summit a relative motion of approach. At the same time a small brilliant spike, giving a broad, bright *Hα* line, was seen on the disk between the two members of the preceding spot.

At $11^h\ 12^m$ the slender prominence, now apparently higher, was forked, as in *A*, Figure 19. Five minutes later the fork had vanished, and the prominence appeared nearly as in Figure 18 at the center of *Hα*; a faint slender arc (*C*, Fig. 19), directed toward the second member of the preceding pair of spots, was also seen to the north. When the line-shifter was turned to admit longer wave-lengths, another slender linear prominence (*B*, Fig. 19) appeared well toward the red. These fleeting phenomena were gone before they could be carefully measured and sketched. At $11^h\ 42^m$ two linear prominences could be seen, as indicated in Figure 20. The southern (*A*)

was of maximum intensity near the middle of $H\alpha$ (about $+3$), while the maximum brightness of the northern one (B) was at -24, where A was not visible. Similar intermittent phenomena, changing as

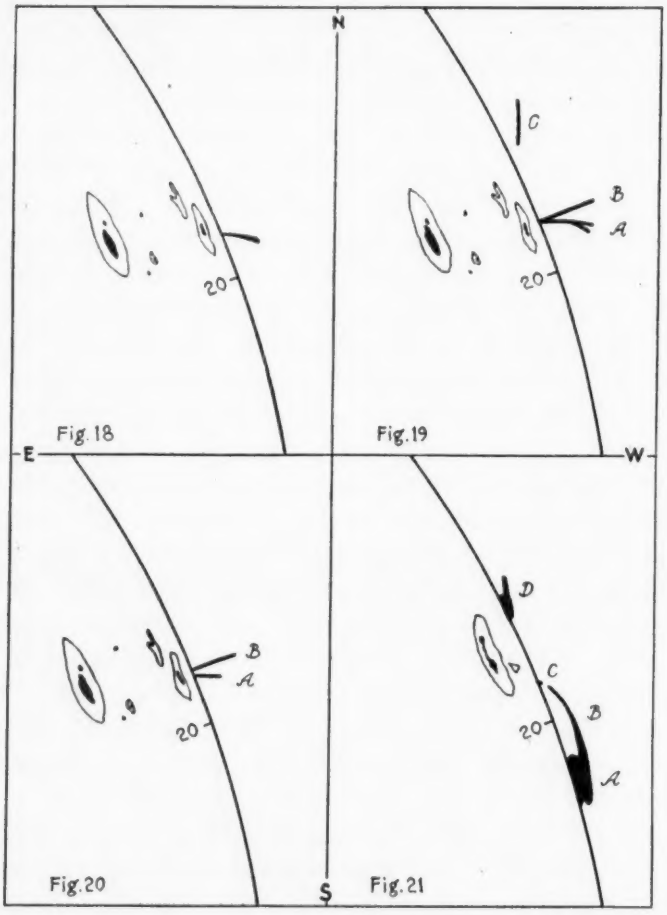

FIGS. 18, 19, 20.—Prominences observed on September 24, 1926, near preceding spot of Mt. Wilson No. 2686.

FIG. 21.—Prominences observed on September 26, 1926, between spots of Mt. Wilson No. 2686.

rapidly in intensity and radial velocity, were observed later in the morning, in spite of a very thick atmosphere, the forerunner of a fog.

On September 26, as Ellerman's polarity sketch at $6^h\ 40^m$ shows,

the preceding spots of the bipolar group were beyond the limb, while the following spot was approaching it. I cannot attempt to illustrate the rapidly changing prominences seen at the limb with the spectrohelioscope on this date, but Figure 21 will serve roughly to indicate the general character of the most significant of them. At $10^h\ 27^m$, after a heavy ground fog had cleared away, I saw at *A* a comparatively low prominence, which already extended toward the spot nearly to *B*, with a minute pointlike tip in advance of the slender extension behind it. About fifteen minutes later the tip had curved down to meet the limb not far from *C*. At this moment I noticed a short bright eruptive spike *D* just north of the spot, characterized by a very broad *Hα* line. I tested the image of the spike given by the edges of this bright line with a nicol prism and half-wave plate, but could detect no evidence of polarization. At $11^h\ 03^m$ the prominence *A* was nearly twice as high as when first seen, but the slender extension *BC* toward the spot had disappeared. Meanwhile, the spike *D* had thrown out toward the north an intensely bright extension, partly overlapped by a bright arch, which had enlarged and grown fainter as it moved away from the spot. At $11^h\ 10^m$ the prominence *A* had begun to develop a new slender extension advancing toward *B*, while an arch overlapping *D* (not shown in Fig. 21) had brightened and lengthened toward the north. Its brilliant top had little or no radial motion, but its lower end, which now curved down nearly to the limb, showed a rapid velocity of recession. At $11^h\ 35^m$ the extension from *A* reached beyond *B* and another smaller prominence similar in form to *ABC* had appeared beneath it. Other changes had occurred, including the formation of an arch extending south from above the spike *B*, with which it seemed to have no connection. Similar rapid changes continued, but at $12^h\ 20^m$ little remained excepting two low prominences at *A* and *D*.

On September 27 a prominence closely similar to *ABC* in Figure 21 was seen at $10^h\ 40^m$, near the same position angle. This is a typical form near sun-spots, which I have often observed with the spectrohelioscope. In our photographic records it goes back as far as my early wide-slit photographs of a prominence with the K line of calcium, made at the Kenwood Observatory, Chicago, on October

20, 1891,[1] and the three successive photographs of a prominence, showing the growth of its long slender extension, taken at Kenwood with my first spectroheliograph in 1893 (Plate VII*a*, *b*, *c*). Other Kenwood negatives and many made with the 40-inch Yerkes telescope and the Rumford spectroheliograph show prominences of the same type, some of which have been mentioned in references to the work of Slocum and Pettit.

It is not my purpose to enter here into a detailed examination of the observations described above, as these will be supplemented by other observations and discussed in my next paper on whirls and arches in the solar atmosphere. I wish, however, to emphasize a few conclusions bearing on the effective use of the spectrohelioscope and the nature of the phenomena it discloses.

1. As remarked in one of my early papers on the spectroheliograph, in cases of considerable local motion in the line of sight "the portion of a prominence moving with sufficient radial velocity to produce so large a displacement (i.e., great enough to throw the line completely off the second slit) would not appear in the photograph."[2] This accounts for the absence of large and often very significant portions of prominences and flocculi from spectroheliograms, and illustrates the value of the spectrohelioscope for the study of such phenomena.

2. On the other hand, as such photographs as those reproduced in Plates IV, V, and VI indicate, the spectroheliograph is incomparably superior to the spectrohelioscope for recording most of the intricate details of the *Hα* fields of force surrounding sun-spots. My rough schematic sketches hurriedly made with the latter instrument make no pretense to accuracy, but will serve to show the nature of the velocity analyses of certain outstanding phenomena.

3. The advantages and disadvantages of the spectrohelioscope for velocity measures and thus for the analysis of the flocculi should be borne in mind while observing. Its limitations depend upon the width of the second slit, the dispersion employed, and the nature of the intensity-curve of the *Hα* line. It is important to remember, as already stated, that a flocculus may be seen even when the second

[1] *Astronomy and Astrophysics*, **11**, 77, 1892.

[2] "The Spectroheliograph," *Astronomy and Astrophysics*, **12**, 256, 1893.

PLATE VII

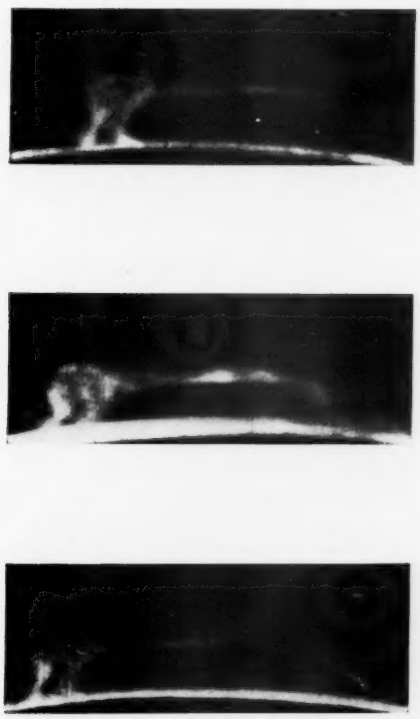

THREE SUCCESSIVE PHOTOGRAPHS OF A PROMINENCE
Taken with the Kenwood Spectroheliograph (K line) in 1893

UNIV. OF MICH.

slit of the spectrohelioscope falls near the extreme outer edge of its *Hα* line, though it may be very faint under these conditions. On this account, and in view of the fact that the intensity-curve of the line may be materially altered by the physical condition of the absorbing or radiating hydrogen, caution must always be observed in interpreting the results. In general, however, the circle of the line-shifter, when set for a position of maximum intensity, affords a quick and dependable means of analysis.

CARNEGIE INSTITUTION OF WASHINGTON
MOUNT WILSON OBSERVATORY
January 1930

LUNAR RADIATION AND TEMPERATURES[1]

By EDISON PETTIT and SETH B. NICHOLSON

ABSTRACT

Methods of observing.—The vacuum thermocouple attached to the 100-inch telescope was used as in measuring stellar radiation. A microscope cover-glass was used to separate the reflected light from the planetary heat. A fluorite screen and water-cell were used for special purposes.

Reduction of the measurements.—Comparison stars, whose radiometric magnitudes we have already determined, were used to reduce the galvanometer deflections to absolute intensities. These are expressed in terms of the radiometric magnitude of the planetary heat in a solid angle of 1 sq. sec. of arc. The relation of radiometric magnitude to absolute temperature is given by the equation

$$\log T = 2.612 - 0.1\,(\bar{m}_r - \Delta m_r)\,.$$

An expression applicable to the screens used and to the conditions of observing is derived from this equation.

Limiting measurable temperature.—Temperatures below 100° K are measured with difficulty, since the value of m'_r for that temperature is 12.47 mag.; and it is probably not feasible to detect planetary radiation from a celestial body whose temperature is below 70° K.

Reflection of solar radiation between 8 and 14 μ.—Even if the moon reflected all the solar radiation in this region, it would add only 1½ per cent to the planetary heat and affect the computed temperature by only 1°. With the fluorite screen the emissivity between 8 and 10 μ is shown to be the same as between 8 and 14 μ, which indicates that the silicates, if present in the lunar crust, cannot be detected by the selective emissivity between 8 and 10 μ as in laboratory tests, probably because they are in a finely divided or porous state for which the emissivity would be more like that of a black body.

Distribution of radiation over the disk.—From drift-curves it is found that the distribution of planetary heat over the disk at full moon does not follow the formula

$$E = a \cos\theta\,,$$

derived from the Lommel-Seeliger law, but more nearly the formula

$$E = a \cos^{3/2}\theta\,.$$

This is explained by the rough surface. From the water-cell drift-curve it appears that the general trend of reflected light at full moon is uniform, but that at the limb in the E.–W. direction the intensity is 60 per cent greater than that of the neighboring *maria*.

Temperature of the subsolar point.—The measures indicate that at full moon, when the subsolar point is nearly central on the disk, its temperature is 407° K, but that at quarter-phase, when it is on the limb, they show a temperature of 358° K. The directive effect of the rough surface on the planetary heat probably accounts for this difference.

Temperatures during a lunar eclipse.—Measurements made near the south limb on June 14, 1927, show that the temperature fell from 342° to 175° K during the first partial phase, continued to drop to 156° K during totality, and rose again abruptly to nearly the original temperature during the last partial phase. From these data it is estimated that less than 0.1 cal cm^{-2} min^{-1} is conducted into the moon from the surface.

Distribution of planetary heat and reflected light about the subsolar point.—With special equipment the night-to-night values of the reflected light transmitted by the cover-

[1] *Contributions from the Mount Wilson Observatory, Carnegie Institution of Washington*, No. 392.

glass and of the planetary heat eliminated by it were determined for the subsolar point as it passed over the earthward side of the moon. The mean spherical distribution of light over the hemisphere about the subsolar point is 0.85 mag. fainter and the planetary heat 0.15 mag. fainter than the corresponding intensities at full moon.

The theoretical lunar temperature.—From the water-cell measurements and the distribution-curve, the light reflected from the subsolar point is estimated to be 0.24 cal cm^{-2} min^{-1}; and combining this with the amount conducted and with the solar constant, we find the mean spherical rate of lunar emission to be 1.61 cal cm^{-2} min^{-1} and the computed black-body temperature to be 374° K. From the distribution-curve of planetary heat about the subsolar point the mean spherical rate of emission is found to be 1.93 cal cm^{-2} min^{-1} and the corresponding temperature 391° K, which is to be compared with the theoretical temperature of 374° K.

Atmospheric absorption.—A discussion of the discrepancy between the observed and theoretical rate of lunar emission gives a set of corrections to the atmospheric absorption constants, derived on the assumption that the entire difference is due to errors in these quantities.

Reflection of solar radiation from the lunar surface.—From the distribution-curve of reflected light about the subsolar point and the drift-curve made with the water-cell in the beam the formula

$$E_r = K \frac{0.46 \sec^2 i/2}{0.46 \cos \theta + \sin \theta} \qquad (22)$$

was derived, where i and θ are the angles of incidence and reflection, respectively. The laws of Lambert, Lommel and Seeliger, and Euler cannot be made to fit the observational material.

Radiometric albedo.—The radiometric magnitude of the reflected light is found to be −13.3, and of the whole lunar radiation −14.8. The radiometric albedo of the reflected light is 0.093.

Temperature of the dark side.—This was found to be 120° K. The temperature is so low that considerable observing will be necessary to establish a good value.

The radiation from a planet consists of two parts: reflected sunlight which, when it reaches us, is confined practically to the limits of wave-length 0.3 to 5 μ, and the low-temperature radiation called "planetary heat," which is emitted by the warmed surface and which reaches us principally through the great water-vapor transmission band between 8 and 14 μ. The small amount of planetary heat transmitted between 0.3 and 8 μ is nearly negligible except in the case of the planet Mercury. To separate these radiations a microscope cover-glass 0.165 mm thick is superior to a water-cell, since any errors in the spectral reflection coefficients for the planet enter into the results very much less with the former screen than with the latter.

TRANSMISSION COEFFICIENTS

The transmission-curves of the microscope cover-glass,[1] water-cell,[1] fluorite screen,[2] rock-salt window,[2] and the atmosphere[3] are

[1] *Mt. Wilson Contr.*, No. 336; *Astrophysical Journal*, **66**, 43, 1927.

[2] *Smithsonian Physical Tables* (7th ed.), p. 305, 1921.

[3] *Smithsonian Miscellaneous Collections*, **68**, No. 8, 1917.

shown in Figure 1. All of these are well determined except that of the atmosphere. The only complete data on the transmission of water vapor and the atmosphere in long wave-lengths where planetary heat is radiated most abundantly are those obtained by F. E. Fowle.[1] The admirable experimental data from which these transmission coefficients were determined covered the range 0.001 to 0.082 cm of precipitable water, whereas the amount between an observer on Mount Wilson and a celestial object in the zenith is 0.7

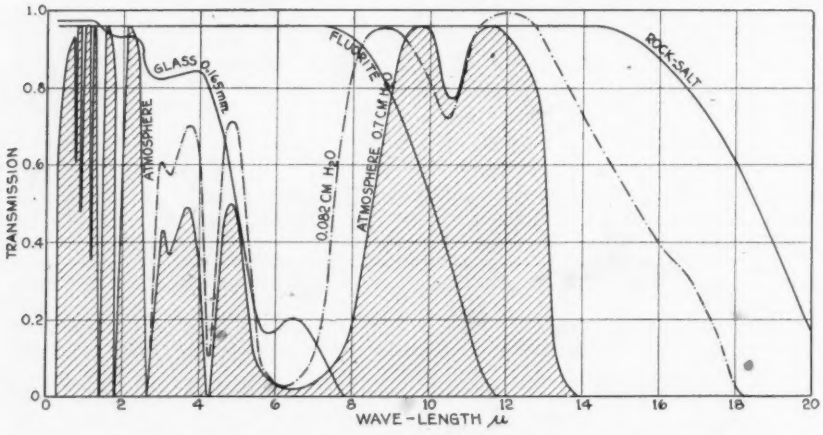

FIG. 1.—Transmission curves of (*a*) the atmosphere above Mount Wilson (the shaded curve); (*b*) water vapor 0.082 cm precipitable water; (*c*) microscope coverglass, 0.165 mm thick; (*d*) fluorite 4 mm; and (*e*) rock salt 2 mm.

cm,[2] which necessitates an extrapolation of the observational data over a range 900 per cent greater than that observed. Probably no greater contribution to our knowledge of planetary temperatures could be made than a determination of the transmission coefficients of water vapor between 2.7 and 20 μ for amounts in the neighborhood of 1 cm of precipitable water, which is equivalent to a column of steam 16.7 m long at normal atmospheric pressure.

The shaded curve in Figure 1 is that for the atmosphere having 0.7 cm of precipitable water as recommended by Fowle,[3] with details

[1] *Ibid.*, p. 23, 1917.

[2] *Astrophysical Journal*, **35**, 149, 1912; *Annals of the Astrophysical Observatory, Smithsonian Institution*, **3**, 171, 1913.

[3] *Smithsonian Miscellaneous Collections*, **68**, No. 8, 1917.

in the near infra-red from radiation-curves which we observed for the purpose. That portion of the curve between 2 and 14 μ was made as nearly symmetrical as possible with Fowle's laboratory curve (the broken line) for 0.082 cm of precipitable water, the data for which are given in his table only in steps of 1 μ.

Variation in the amount of atmospheric water vapor will, of course, affect the atmospheric transmission. According to the shaded curve, a variation of 50 per cent[1] in the water vapor changes the transmission of the atmosphere 11 per cent. The formula of Hann,

$$p = 1.7\, e_w \sec z, \qquad (1)$$

gives the precipitable water p in the optical path for a given vapor pressure e_w. Fowle[2] has shown that in actual practice the coefficient 1.7 varies over a large range. On account of this and the uncertainty in the transmissions themselves it was thought better not to include observations when p differed largely from the mean value 0.7 cm than to apply corrections which could be of little certainty. From Fowle's extrapolations, which apply to the shaded curve only, it follows that the correction due to a variation of p, to be applied to a galvanometer deflection, B, for planetary heat from a celestial object between 300° and 500° K, is

$$\delta B = \frac{p - 0.7}{3} B, \qquad (0.3 < p < 1.5 \text{ cm}). \qquad (2)$$

OBSERVATIONAL DATA

The general method which we have used for measuring radiation from celestial objects has already been discussed.[3] The vacuum thermocouple employed for most of the lunar observations had a silver shield covering all the thermocouple and the platinum lead-wires except the receiver 0.62 mm square over one junction. The cell of the thermocouple was provided with a rock-salt window 2 mm thick.

[1] See also *Annals of the Astrophysical Observatory, Smithsonian Institution*, **4**, 284–285, 1922.

[2] *Astrophysical Journal*, **35**, 149, 1912; *Annals of the Astrophysical Observatory, Smithsonian Institution*, **3**, 171, 1913.

[3] *Mt. Wilson Contr.*, No. 369; *Astrophysical Journal*, **68**, 279, 1928.

The general scheme of observing was to make (1) a series of measurements on the moon with the microscope cover-glass, water-cell, and fluorite screen, and without any screen at all (free deflection); (2) a set of free deflections on a star whose radiometric magnitude we had previously determined;[1] and (3) a reading of the sling psychrometer. All the measurements were made at the Newtonian focus of the 100-inch telescope, where the mean diameter of the lunar image is 116.6 mm. The width of the receiver of the thermocouple is only 0.0055 of this image.

REDUCTION OF THE MEASUREMENTS

We have already pointed out[2] that the temperature of a star computed from the total radiation is given by

$$\log T = 2.638 - 0.1\,(m_r - \Delta m_r) - \tfrac{1}{2}\log d\,, \qquad (3)$$

where T is the absolute temperature, m_r the radiometric magnitude, Δm_r the loss, in magnitudes, due to the atmosphere and silvered surfaces of the telescope, and d the diameter of the star in seconds of arc. This formula assumes that the star radiates uniformly over its apparent surface—a condition which is approximately satisfied for the total radiation from the sun. From drift-curves on the sun taken in the Pasadena laboratory we have found that d from (3) should be multiplied by 1.07 for dG-type stars. In the case of a planet, d is the angular diameter of the receiver as seen from the mirror of the telescope, provided that the receiver is so small that the temperature of that part of the disk covered by it is practically constant. If the image of the planet approaches or is smaller than the diameter of the receiver, the condition of uniform distribution of radiation over the receiver no longer holds, and d is then the angular diameter of the receiver, on the one hand, or the angular diameter of the planet, on the other, corrected for distribution of radiation. Since either of these cases may occur for a planet, the last term of equation (3) has been changed to correspond to the diameter of a solid angle of 1 sq. sec. of arc of planetary heat and

[1] *Ibid.*, Table III.

[2] *Ibid.*, equation 4.

all observations have been reduced to this unit. Equation (3) then becomes

$$\log T = 2.612 - 0.1\ (\bar{m}_r - \Delta m_r)\ , \tag{4}$$

where $\bar{m}_r$ is the radiometric magnitude of a solid angle of 1 sq. sec. of arc of planetary heat. This equation gives the temperature corresponding to the mean radiation from the portion of the planet's surface, the image of which falls on the thermocouple, and assumes that the spectral distribution of energy is like that of a black body.

The values of Δm_r (Table I) have been obtained for various temperatures by combining the black-body curves with the atmospheric transmission-curves in Figure 1 and the reflecting power of silver, which for two reflections is 0.97 throughout the region of planetary heat.

The values of $\bar{m}_r$ are obtained from

$$\left.\begin{aligned} \bar{m}_r = m_r + (C-c) + 10/4 \log b - 10/4 \log B \\ -(a \sec Z - 0.16 \sec z) - P + 10/4 \log As^2\ , \end{aligned}\right\} \tag{5}$$

where m_r is the radiometric magnitude of the comparison star, $C-c$ the correction to m_r due to tarnishing of the silver, b the deflection for the star, B that part of the deflection for the planet due to planetary heat, Z and z the zenith distances of the moon and the star, respectively, a the coefficient of atmospheric extinction for planetary heat, P the correction in magnitudes from equation (2) due to the deviation of the water-vapor content of the atmosphere from the average, A the area of the thermocouple receiver in square millimeters, and s the scale of the telescope field in seconds of arc per millimeter. We will consider these quantities in the order in which they occur in equation (5).

The values of m_r for a number of stars have already been published.[1] The correction to m_r due to the differential absorption of radiation from the star and planetary heat by tarnished silver is

$$C-c = D\ (S_p - S_s)\ , \tag{6}$$

[1] *Ibid.*, Table III.

where D is the number of days since silvering, S_p the coefficient for planetary heat, and S_s the coefficient for the comparison star. S increases with spectral class[1] but becomes nearly constant at 205×10^{-6} mag. per day for the radiation from M-type stars, and, since planetary heat is of still longer wave-length, we may substitute this value for S_p in equation (6).

In obtaining B, that part of the deflection due to planetary heat, the free deflection, F, is combined as follows with Cg, the deflection observed with the cover-glass screen. Let R be that part of the light reflected from the planet, Tr the transmission of planetary heat through the cover-glass, and tr the transmission of the reflected light from the planet through the cover-glass. Then,

$$F=B+R\,, \tag{7a}$$

$$Cg=BTr+Rtr\,, \tag{7b}$$

$$B=\frac{F-\dfrac{Cg}{tr}}{1-\dfrac{Tr}{tr}}\,. \tag{7c}$$

The coefficient, a, of sec Z was determined from a series of measurements on the moon and Mars which gave a value of 0.16 mag., the same as the mean value for stellar radiation.

P is equivalent to δB in equation (2) expressed in magnitudes, and $s^2=256$ sq. sec. of arc at the Newtonian focus of the 100-inch telescope.

For planets in general we substitute B from equation (7c) into equation (5) and obtain (8):

$$\left.\begin{aligned}\bar{m}_r=m_r&+D(205\times 10^{-6}-S_s)+10/4\log b-10/4\log\left(F-\frac{Cg}{tr}\right)\\&+10/4\log\left(1-\frac{Tr}{tr}\right)-0.16\,(\sec Z-\sec z)-10/4\log\frac{p+2.3}{3}\\&+10/4\log As^2\,.\end{aligned}\right\} \tag{8}$$

[1] *Ibid*, Table I.

If we substitute the value of $\bar{m}_r$ from (8) into equation (4) and collect the constants and those variables which are functions of the planetary temperature, T, we obtain

$$\left.\begin{aligned} m_r+D\,(205\times10^{-6}-S_s)+10/4\,\log b-10/4\,\log\left(F-\frac{Cg}{tr}\right)\\ -0.16\,(\sec Z-\sec z)-10/4\,\log\frac{p+2.3}{3}+10/4\,\log As^2\\ =26.12-10\,\log T+\Delta m_r-10/4\,\log\left(1-\frac{Tr}{tr}\right)=m_r'\,, \end{aligned}\right\} \quad (9)$$

which applies to any planet for which the spectral distribution of the reflected light is known. This equation represents the radiometric magnitude of the planetary heat eliminated by the cover-glass for a solid angle of 1 sq. sec. of arc; the second member can be calculated for any planetary temperature, T, and the first member, which will be called m_r', can be obtained from observations.

It has already been shown[1] that, in the visible spectrum at least, the energy-curve of moonlight gives a color-index on the Mount Wilson scale[2] of 0.92 mag., which corresponds approximately to that of a K0 dwarf star. The absorption of the cover-glass screen for a star of this type[3] is 0.03 mag. with sufficient approximations, and the radiation reflected by it is 0.08 mag. Hence, the value of tr for the moon is 0.90. Substituting this value of tr into equation (9), we have equation (10), which applies to observations of the moon:

$$\left.\begin{aligned} m_r+D\,(205\times10^{-6}-S_s)+10/4\,\log b-10/4\,\log\,(F-1.11Cg)\\ -0.16\,(\sec Z-\sec z)-10/4\,\log\frac{p+2.3}{3}+10/4\,\log As^2\\ =26.12-10\,\log T+\Delta m_r-10/4\,\log\,(1-1.11Tr)=m_r'\,. \end{aligned}\right\} \quad (10)$$

From the atmospheric transmission-curves in Figure 1, the black-body energy-curves for various temperatures, and the reflecting power of silver, we have computed Table I for different values of T. The application of $\Delta m_r'$ will be discussed later.

In equation (10) the first and third terms of the left-hand mem-

[1] *Publications of the Astronomical Society of the Pacific*, **38**, 242, 1926.

[2] *Mt. Wilson Contr.*, No. 226; *Astrophysical Journal*, **55**, 165, 1922.

[3] *Mt. Wilson Contr.*, No. 369; *Astrophysical Journal*, **68**, 279, 1928.

ber are fixed by the conditions of observing. The correction due to tarnished silver given by the second term did not exceed 0.05 mag. The reduction for air mass given by the fifth term did not exceed 0.16 mag. The correction for atmospheric water vapor given by the sixth term would not have exceeded 0.1 mag. The last term, which depends on the area of the thermocouple receiver and the scale of the telescope, was 5.07 mag. for the thermocouple previously described when used at the Newtonian focus of the 100-inch reflector.

TABLE I

T	Δm_r	Tr	m'_r	$\Delta m'_r$
100° K	6.35	0.000	+12.47	−0.49
150			7.80	.38
200	2.12	.000	5.23	.28
250			3.76	.24
300	1.39	.013	2.76	.20
350			2.01	.19
400	1.28	.063	1.45	.18
450			0.99	.18
500	1.28	.147	.60	.18
550			+ .27	.17
600	1.30	.249	− .01	.17
650			.25	.17
700	1.31	.364	.46	.17
750			.67	.16
800	1.25	0.468	− 0.85	−0.16

The lower limit of planetary temperature which can be measured is fixed by the sensitiveness of the thermocouple circuit and the area of the receiver, if the receiver is smaller than the image of the planet. As has been pointed out,[1] stars of radiometric magnitude +7 can be observed with the routine equipment which we have used; and with especially constructed thermocouples a gain of two additional magnitudes can be made. By adding the last term of equation (8) for the thermocouple described above, planetary heat of radiometric magnitude +12 could be measured with an accuracy of about 10 per cent, and with effort this might be increased to +15 or +16 if a large surface were available. Table I shows that planetary heat eliminated by the cover-glass of radiometric magnitude

[1] *Ibid.*

+12 corresponds to a temperature of 100° K, and of magnitude +16 to 70° K. From this it is seen that the temperatures of celestial objects much below 100° K can be determined only with difficulty.

REFLECTION OF SOLAR RADIATION OF WAVE-LENGTH 8–14 μ

It is well known that silica and to a less extent the silicates, of which the lunar crust may contain a large percentage, have high reflecting power in the region 8–14 μ. If these substances are present, it might be supposed that the solar radiation reflected from the lunar surface would be great enough to affect the temperatures calculated on the assumption that all the radiation in these wave-lengths is planetary heat radiated by the warmed surface of the moon. A simple calculation from Planck's black-body formula shows, however, that the reflected solar radiation would be less than 1½ per cent of the planetary heat, even if the reflecting power of the lunar surface were perfect over the whole atmospheric transmission band 8–14 μ. This would decrease the computed temperature about 1°, which is less than the uncertainty arising from other sources. It is not easy, therefore, to determine by this means whether the lunar crust has a high silicate content.

Since the emissivity of silica (and to a less extent of the silicates) is abnormally low between 8 and 10 μ,[1] some indication of its presence should be revealed by the transmission of planetary heat through a fluorite screen, which, as an examination of Figures 1 and 2 will show, isolates just this spectral region. We will now compare the ratio, H, of the observed planetary heat transmitted by the fluorite screen to that without a screen and the similar ratio computed (*a*) by assuming unit emissivity and (*b*) by assuming the emissivity to be that of silica. From the curves in Figure 1 it will be seen that this ratio is essentially that of fluorite *minus* cover-glass to free deflection *minus* cover-glass, or of the energy between 8 and 10 μ to that between 8 and 14 μ.

From drift-curves in Figure 3 we find the following data, which

[1] Wood, *Physical Optics*, p. 602, 1911; Sosman, *The Properties of Silica*, p. 738, 1927.

apply to the subsolar point where the temperature is approximately 400° K:

$$F = 145 \text{ mm},$$
$$Fl = 79 \text{ mm},$$
$$Cg = 41 \text{ mm},$$
$$H = \frac{Fl - Cg}{F - Cg} = 0.37,$$

where Fl is the deflection with the fluorite screen in place.

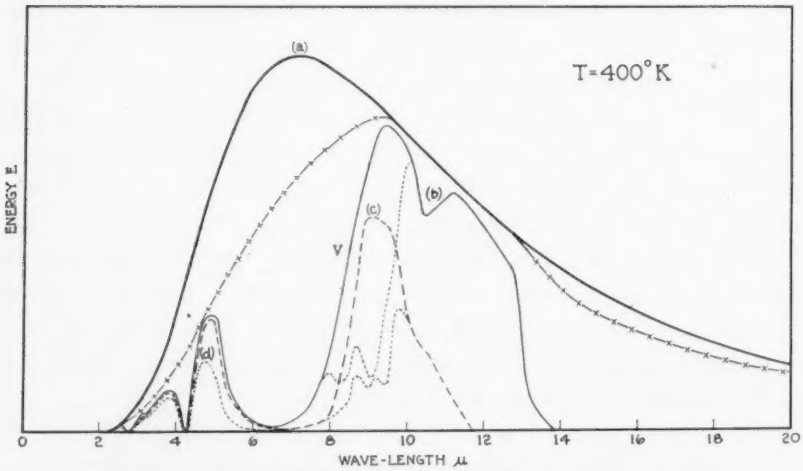

FIG. 2.—Energy-curve (*a*) of a black body at 400° K; (*b*) the same after the radiation has passed through the earth's atmosphere, the dotted line between 8 and 10 μ being the deformation due to presence of silica; (*c*) after passage through fluorite screen, the dotted line between 8 and 10 μ being the deformation due to presence of silica; (*d*) after passage through microscope cover-glass (red limit at 6 μ). The dash-and-cross line is the deformation of (*a*) necessary to explain the discrepancy between the observed and theoretical lunar temperatures.

From these data it can also be seen that the reflected light, R, which is essentially represented by Cg, is 0.39 as great as the planetary heat represented by $F - Cg$.

From the ordinates of the curves in Figure 1 multiplied into those of a black body at 400° K, we obtain Figure 2, where (*a*) is the spectral energy-curve for a black body at 400° K, (*b*) the same after transmission by the atmosphere, (*c*) after further transmission by the fluorite screen, and (*d*) after transmission by the cover-glass.

From this we find that the area which represents planetary heat in the free deflection is 2054, and that when the fluorite screen is in place it is 773. The ratio of these numbers represents H approximately, but to get a more exact value we must apply equations (7*a*) and (7*b*), which allow for the small amount of planetary light lost by the cover-glass. From these we find

$$Fl-Cg=0.05R+\ 773\,,$$

$$F-Cg=0.10R+2054\,,$$

whence

$$H=\frac{Fl-Cg}{F-Cg}=\frac{41+\ 773}{82+2054}=0.38\,,$$

where R is taken at 0.39 Cg as above, and the reflecting power used for fluorite is 0.05. While the observed value $H=0.37$ is less than the 0.38 computed from the transmissions on the assumption of equal emissivities in the regions 8–10 μ and 8–14 μ, it can scarcely be interpreted as implying the presence of silicates, since with such a close agreement no surprise would have been caused had the figures been interchanged. From this, together with the nature of the lunar surface indicated by the low conductivity as shown in the discussion of eclipse observations to follow, it appears that practically all the planetary heat in the region 8–10 μ is accounted for by the assumption of unit emissivity.

We will now compute H on the assumption that the moon has a relatively smooth silica surface. The computed spectral energy-curves of planetary heat transmitted by the atmosphere and by the fluorite used above must be multiplied by the emissivity coefficients of silica before the ratio H is determined. The adopted coefficients, e, are as follows:[1]

λ	e	λ	e
7.75 μ	1.00	9.0 μ	0.20
8.0	0.76	9.25	.24
8.25	.38	9.5	.42
8.5	.30	9.75	.68
8.62	.40	10.0	0.98
8.75	0.32	10.25	1.00

[1] *Ibid.*

From these data we find

$$H=\frac{41+505}{82+1691}=0.30\,.$$

This value of H is so radically different from the observed value that we conclude that the emissivity of the lunar surface in the region 8–10 μ is unity for practical purposes and unaffected by any silica content it may have. This does not necessarily mean that the silica content of the lunar crust is small, for if it were finely divided like sand or porous like pumice, which probably would be its state if present, its radiating properties would be nearly those of a black body.[1] We can only say then that if silica or silicates are present, they are probably in the finely divided or porous state. It is possible that spectroscopic examination of the violet slope V (Fig. 2) of the band at 8–14 μ might reveal a deformation due to the emissivity of small amounts of non-porous silicates which would escape detection by the foregoing methods. It will be recalled, however, that the energy-curve[2] of lunar radiation obtained by Langley and Very showed no effect of this kind.

DISTRIBUTION OF RADIATION OVER THE DISK

Figure 3 shows drift-curves along a parallel of declination passing through the center of the disk of the full moon on June 16, 1924, when the phase angle was 0°. The curves were made by unclamping the telescope and allowing the image of the moon to transit the thermocouple. They represent (1) free radiation, that is, without filters, (2) radiation transmitted by 4 mm of fluorite, (3) radiation transmitted by 0.165 mm of glass, and (4) radiation transmitted by 1 cm of water. Number 1 represents all the planetary heat and all the reflected light transmitted by our atmosphere and reflected by the telescope mirrors. Number 2 represents about 35 per cent of the planetary heat and about 90 per cent of the reflected light. Number 3 represents about 11 per cent of the planetary heat and about 95 per cent of the reflected light, while No. 4 represents about 60 per

[1] *Ibid.*, p. 740.

[2] *Memoirs of the National Academy of Sciences*, 4, Part II, 193 ff., 1889.

PLATE VIII

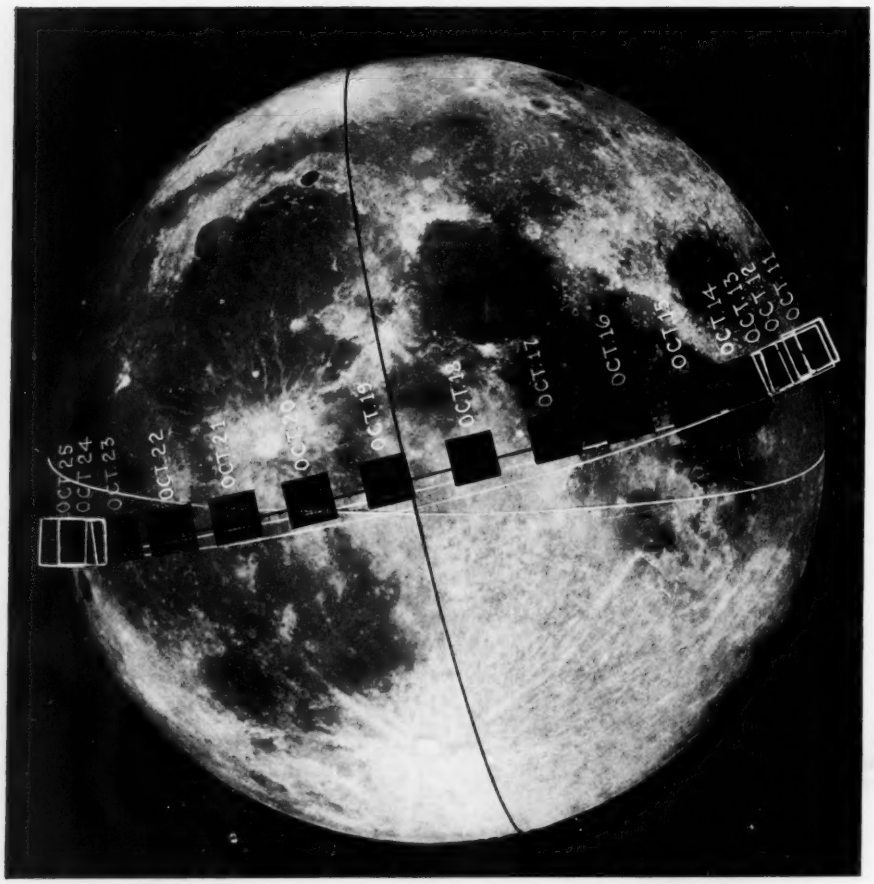

The white lines represent the width of path traversed by the thermocouple-receiver in recording drift-curves such as in Figure 3; the black lines are the axes of lunar co-ordinates. The black squares represent the size and position of the receiver in measuring the energy from the subsolar point between first and last quarters. These measures were used to obtain the distribution-curves in Figure 7.

UNIV.

cent of the reflected light. The principal features of the moon corresponding to points on the curve are indicated below.

Plate VIII is a photograph of the full moon made at the Lick Observatory, upon which are plotted the axes of co-ordinates (in

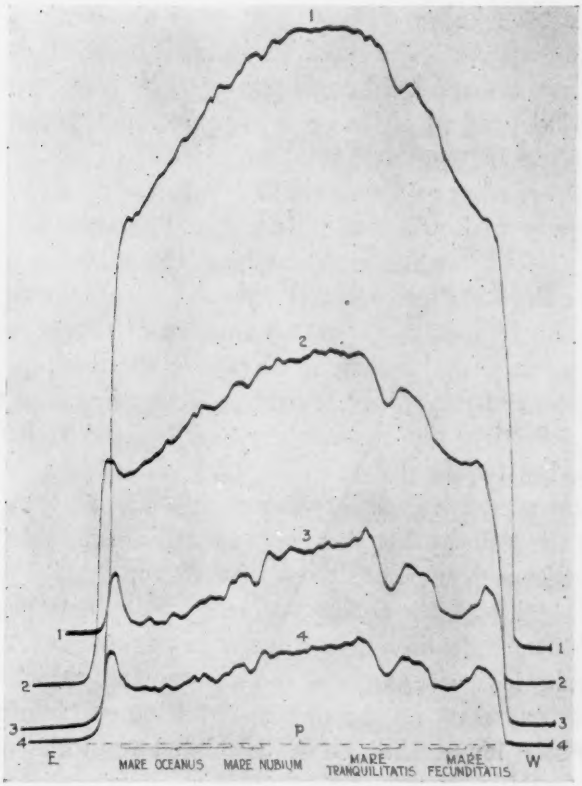

FIG. 3.—Drift-curves across full moon: (1) free radiation; (2) fluorite screen; (3) cover-glass; (4) water-cell.

black) and the paths (in white) traversed by the thermocouple junction on the three dates when drift-curves were taken. The width of the white lines is that of the thermocouple-receiver as used at the 100-inch telescope in making the drift-curves. The black squares refer to the dimensions of the thermocouple-receiver as used at the Snow telescope in the focus of a 27-inch mirror of 67 inches focal

length in the study of the distribution of energy about the subsolar point to be described later. We will first discuss the distribution of planetary heat over the disk.

DISTRIBUTION OF PLANETARY HEAT OVER THE DISK

As has been known from experimental observations for more than a hundred years, the radiation incident on the thermocouple-receiver from a given solid angle presented by a uniformly heated surface is independent of the angle of projection.[1] If we consider a smooth sphere, not in rapid rotation, exposed to parallel sunlight, the amount of solar radiation which is incident on and can be absorbed by any small-unit area and converted into heat will vary with the cosine of its angular distance from the subsolar point. The amount of planetary heat radiated by the small area in any directed unit solid angle, if it is a constant fraction of that absorbed, will follow the same law. Hence, if we pass a thermocouple junction over an image of this sphere as seen from any direction, the galvanometer deflections due to planetary heat emitted by it will follow the cosine law (eq. [13])

Two circumstances modify this principle as applied to the moon. The increasing absorption, Δm_r, of the earth's atmosphere for planetary heat from the moon as the receiver moves away from the subsolar point, due to the falling temperature, causes the deflection observed toward the limb or terminator to be too low. A more serious difficulty is the roughness of the lunar surface, which makes the deflections anywhere on the disk near full moon higher, but near quarter-phase lower, than those calculated from the cosine law. The first consideration is obvious from an examination of Table I, but the second may need added explanation.

Two factors which unfortunately cannot be separated appear to explain the effect of roughness. Consider a cavity or bowl-shaped crater. Reflection of planetary heat from the interior by the sides of this depression, or re-emission of absorbed radiation, will tend to make the radiation toward the selenographic zenith greater, and toward the horizon less than it should be, thus making deflections at the center of the disk higher and at the limb lower than the cosine

[1] *Mémoires de l'Académie des Sciences, Paris*, **5**, 179–213, 1826.

law predicts. Again, if we consider an almost vertical mountain side near the terminator and facing the sun, it is clear that its temperature ought to be equal to that of the subsolar point, and its radiation, measured at full moon with a thermocouple-receiver smaller than its image in the field of the telescope, will give the same deflection as that from the subsolar point. At quarter-phase, however, such a mountain face at the terminator is invisible, and the area covered by its shadow will give no deflection. Thus arises the idea of directional temperature. The thermocouple measures the mean radiation of a small area of the moon as seen from the particular direction of the earth at the time, and this is interpreted in terms of temperature. Viewed from a different direction, the mean surface involved would not be the same because of its rough character.

The apparent distribution of planetary heat over the lunar surface can be obtained from the ordinates of curves Nos. 1 and 3 in Figure 3 by applying equation (7*c*) where $tr = 0.90$. The distribution of temperature can be obtained from equation (10). The real distribution of planetary heat over the lunar surface can be obtained from the distribution of temperature. This has been done for plates taken on April 19 and June 16, 1924, and June 14, 1927. The measurements were made for points located at intervals of 0.025 diameter of the apparent disk, and were plotted after reducing the positions of the measured points to the positions they would have for equatorial phase angle 0° when the subsolar point is on the hour circle passing through the center. This may be done by the usual formulae for the measurement of positions on a sphere; but, since the paths in every case pass very close to the subsolar point, the simpler formula of projection in one plane applies:

$$Y = \sin(\sin^{-1} Y_o - i_o), \qquad (11)$$

where Y is the distance in lunar radii from the subsolar meridian, Y_o the observed distance from the central meridian in the same units, and i_o the component of the phase angle in right ascension given by $i_o = 180° - (\alpha\odot - \alpha\leftmoon)$. Y and Y_o are positive west of the central meridian.

The results of such measurements are plotted in Figure 4. The

scale of abscissae gives fractional parts of a radius of the lunar disk, the center of which is on the subsolar meridian indicated in the middle of the figure. The scales of ordinates show the galvanometer deflection B in millimeters due to apparent planetary heat, the radiometric magnitude m_r' of a square second of arc of planetary heat eliminated by the cover-glass, the absolute temperature T, and the energy E emitted by the lunar surface in cal cm^{-2} min^{-1}. The temperatures are computed from the data in Table I.

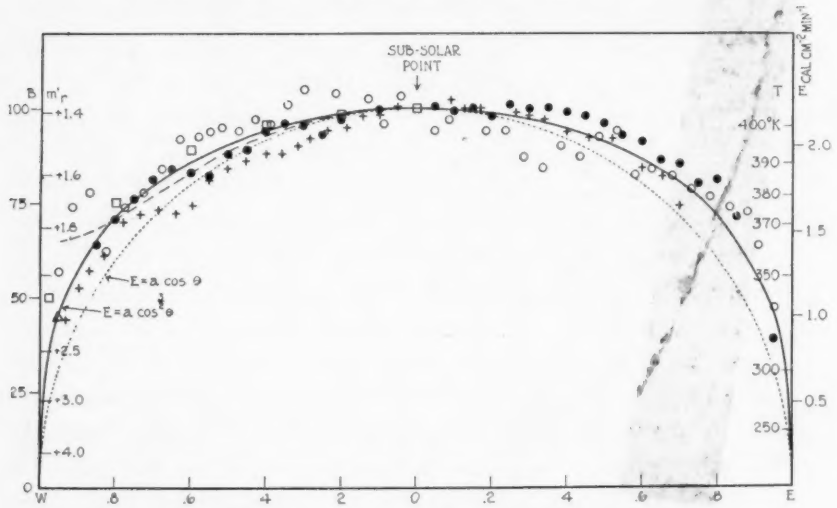

FIG. 4.—Distribution of planetary heat over the disk at full moon

The heavy full line in Figure 4 which represents the plotted observations is also the locus of the equation

$$E = a \cos^{3/2} \theta , \qquad (12)$$

and, as the observed points show, represents the apparent distribution of planetary heat over the lunar disk. An inspection of Figure 4 shows that from the center to 0.95 radius from the center the temperature varies only between 400° and 320° K, and since Δm_r is nearly constant over this range (Table I), the apparent distribution of radiation over most of the lunar surface at full moon is nearly the real one and is practically represented by equation (12).

The semicircle (dotted line) is that which represents the ideal

distribution of planetary heat emitted by a smooth, slowly rotating sphere without atmosphere exposed to sunlight according to the simple formula

$$E = a \cos \theta , \tag{13}$$

where θ is the angular distance of a point from the subsolar point and a is a constant, made equal to the radius of the sphere in this plot.

That roughness of the lunar surface will explain qualitatively, in part at least, the deviation of the drift-curve of planetary heat from the cosine-curve is illustrated by the following simple consideration. If the roughness on the moon is due to non-conducting spheres uniformly distributed over its surface, each sphere will present at full moon a distribution of energy approximating the cosine law, and its radiation in the direction of the earth at that phase will be two-thirds that which the surface it occults would have radiated. It is easily seen then that the energy E emitted in an earthward beam of unit cross-section, small compared to the radius of the moon, will be given by

$$E = E_0 \left[\cos \theta + \frac{na}{k} \left(\frac{2}{3 \cos \theta} - 1 \right) \right] , \tag{14}$$

where E_0 is the energy from the area k in the beam at the subsolar point, θ the angular distance from the subsolar point, n the number of spheres of sectional area a in the area k (at the subsolar point). This equation will hold to a value $\theta = \theta'$, where the spheres would begin to occult each other. The constant na/k was determined from Figure 4 by inserting the observed value of E for $\cos \theta = 0.6$ in equation (14) and was found to be 0.316. From this it appears that the spheres would be separated 3.39 radii, which gives $\theta' = 53^\circ\ 50'$. The locus of this equation appears in Figure 4 as a broken line. An additional point was found for the case where for one orientation of the field the spheres appear mutually tangent, while for another orientation their maximum occultation is 0.78 radius.

In an extended series of measurements during the lunar eclipse of June 24, 1927, a point 0.05 radius from the south limb of the

moon was selected for continuous observation. This gave the point indicated in Figure 4 by a triangle, which agrees fairly well with similar points obtained from the drift-curves above.

DISTRIBUTION OF REFLECTED SOLAR RADIATION OVER THE DISK

Several conclusions concerning the reflected light from the moon follow directly from an examination of curve No. 4 of Figure 3 taken through the water-cell: (*a*) the limb of the moon is 60 per cent brighter than the neighboring surface, which in this case consists of *maria;* (*b*) the center of the moon is 10 to 15 per cent brighter than the limb; (*c*) the brightest point on the E.–W. diameter is on the eastern boundary of Mare Tranquilitatis near longitude 17° W.; (*d*) the *maria* are only three-fourths as bright as the mountainous regions; (*e*) the general trend of the curve is toward uniform brightness, which would be expected from the Lommel-Seeliger or Euler laws of diffuse reflectivity,[1] but not from Lambert's law, which would give a distribution more like that obtained above for planetary heat. A discussion of the laws of diffuse reflection which apply to the moon will be given in another section.

TEMPERATURE OF THE SUBSOLAR POINT

The temperature of the subsolar point has been determined at full moon from the drift-curves described above, and at quarter-phase by observing deflections on the middle of the limb. When the phase angle in the latter case was not exactly 90°, the deflections due to planetary heat were reduced to quarter-phase by equation (13). The results are given in Table II, where m_r^0 is the radiometric magnitude of the moonlight transmitted by the water-cell and the other symbols have the meanings previously defined.

The solar constant has been reduced to the heliocentric distance of the moon at the time of observation, and the average temperatures to 1.93 cal cm^{-2} min^{-1} by the fourth-power law. That the temperature of the subsolar point measured at first quarter is 49° C. lower than that measured at full moon may be explained by the rough surface. The work of Rosse[2] and of Langley[3] showed that the

[1] Müller, *Photometrie der Gestirne*, p. 68, 1897.

[2] *Philosophical Transactions of the Royal Society*, **163**, 587, 1873.

[3] *Memoirs of the National Academy of Sciences*, **4**, Part II, 107, 1889.

lunar temperature was probably as high as boiling water, and the value of 407° K obtained by us for the subsolar point at full moon is in substantial agreement with that found by Menzel[1] from the water-cell observations of Coblentz,[2] the known visual albedo of the moon being used to interpret the eliminated planetary heat in terms of temperature.

TABLE II

TEMPERATURE OF THE MOON'S SUBSOLAR POINT

Date P.S.T.	Solar Const.	Wc.	m_ν^o	m_ν'	T	E
	Full Moon					
1924 Apr. 19	1.92	2.42	+3.44	+1.37	408°K	.....
Apr. 20	1.92	2.50	3.55	1.35	410	.....
June 16	.....	2.01	.....	.....	.....	.....
1927 June 14	1.87	2.00	+3.05	1.44	401	.....
1929 Oct. 17*	1.93	.....	.....	+1.40	405	.....
Corrected average	1.93	2.23	+3.35	+1.39	407	2.24
	Quarter-Phase					
1923 Mar. 24†	1.93	2.49	+4.18	+1.69	377	.....
July 19†	1.85	2.35	3.99	1.96	354	.....
Oct. 14†	1.95	2.30	4.28	2.02	349	.....
Nov. 14†	1.98	2.89	3.80	1.80	367	.....
1924 June 9†	1.90	2.36	4.20	1.81	366	.....
July 24‡	1.88	1.90	+4.05	+2.21	335	.....
Corrected average	1.93	2.38	+4.08	+1.92	358	1.36

* Corresponds to Greenwich Civil date, Oct. 18, on Plate VIII.
† First quarter.
‡ Last quarter.

TEMPERATURES DURING A LUNAR ECLIPSE

A continuous series of measurements of lunar radiation was made during the eclipse of June 14, 1927. A point 48″ (0.05 radius) from the south limb was chosen, since this limb passed nearest to the center of the earth's shadow, the distance at mid-totality being 11′ north. The duration of total phase for this point was 2^h40^m,

[1] *Astrophysical Journal*, **58**, 65, 1923.

[2] *Scientific Papers, Bureau of Standards*, **18**, 535 (No. 438), 1922.

and the partial phases were 1^h each. For the point selected the time of mid-totality was 12^h16^m A.M., P.S.T., which made it a favorable eclipse for continuous measurement. Figure 5 shows the circumstances of the eclipse, P being the position of the thermocouple junction.

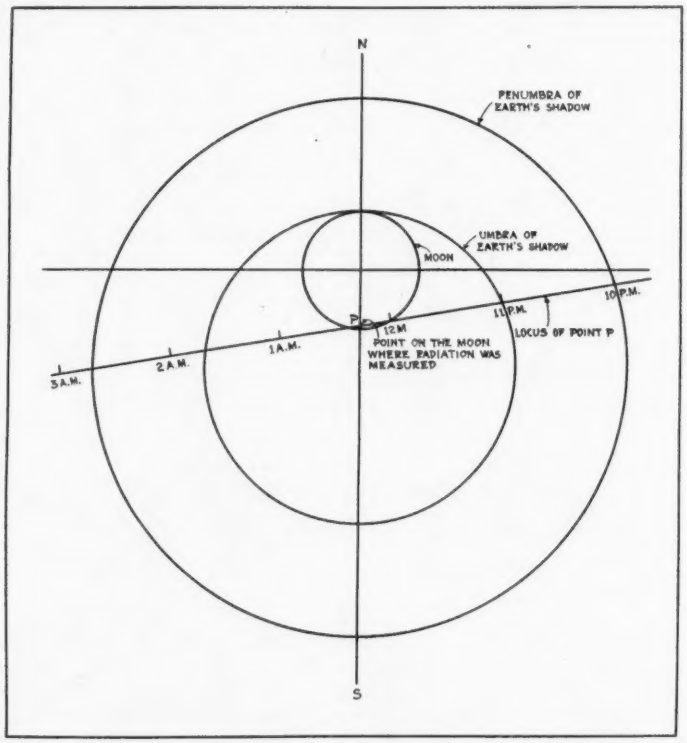

FIG. 5.—Circumstances of the total lunar eclipse of June 14, 1927. The radiation measurements were made at the point P.

The program of observation included several drift-curves before and after eclipse, and deflections on and off the south limb for free radiation, and with the cover-glass and the water-cell in the beam, all taken in the usual manner. Arcturus and Vega were used as comparison stars.

The deflections have been reduced to the zenith as previously described. Since the radiation varied greatly during the eclipse, the

sensitivity used in the electrical circuit was changed in four steps, so that during totality it was 4.2 times as great as before and after the eclipse. The time required to obtain a single set of deflections for free radiation or for that through water-cell or cover-glass was 3 minutes. To simplify the record in Table III the deflections have been read for the same instant from a plot of the observed deflections against the time.

TABLE III

RADIATION DURING LUNAR ECLIPSE

TIME P.S.T.	OBSERVED DEFLECTIONS			m_r'	T	E	E_R
	Free	Cg	Wc				
	mm	mm	mm			cal cm^{-2}	min^{-1}
9^{h}22^m*	617	289	191	+2.09	342°	1.13	1.85
10 04	617	289	182	2.09	342	1.13	1.85
10 30	347	166	113	2.74	300	0.67	1.00
10 52	79.5	33.9	20	4.2	231	.24	0.19
11 13	6.46	1.00	0.80	6.4	174	.08	.00
11 34	4.47	0.07	.64	6.7	170	.07	.00
11 47	5.13	.12	.07	6.5	173	.07	.00
12 02†	2.57	.09	.07	7.3	160	.05	.00
12 28	4.08	.01	.14	6.8	169	.07	.00
12 58	1.48	.20	.16	8.0	149	.04	.00
1 22	2.89	0.42	0.20	7.3	160	.05	.00
1 46	8.92	.....	6.31	7.6	156	.05	.09
1 54	55.0	31.6	21.9	5.0	205	.15	.28
1 59	100	63.1	39.8	4.6	219	.19	0.48
2 28	513	263	174	2.41	320	0.87	1.63
2 41	617	302	200	2.15	339	1.09	1.85
3 04	603	309	204	+2.23	333	1.02	1.85

* P.M. † A.M.

The values of m_r' were computed from equation (10), and the absolute temperatures, T, were read from Table I. E, the radiation emitted by the moon in cal cm^{-2} min^{-1}, was obtained from the black-body formula by using the temperature T. The energy, E_R, received by the moon from the sun, was calculated from the conditions of the eclipse and the distribution of energy on the solar disk.

The total radiation along a radius of the sun is expressed by the formula given by Jeans:[1]

$$\frac{J}{J_0}=0.465+0.535\sqrt{1-r^2}\,, \qquad (15)$$

[1] *Monthly Notices of the Royal Astronomical Society*, **78**, 35, 1917.

where J_0 is the total radiation at the center of the disk and r the distance in radii from the center to the point where the total radiation is J; the constants have been derived from Abbot's data.[1] The total radiation which reaches the moon at any instant as the sun is eclipsed by the earth is the summation over all the uneclipsed area, each element of which is to be weighted according to equation (15). Table IV gives the resulting intensity of solar radiation on the moon as a function of the fraction of a solar diameter occulted by the earth.

TABLE IV

Fraction of Solar Diameter Occulted by Earth	Fraction of Total Solar Radiation Received by Moon
0.1	0.96
.2	.89
.3	.79
.4	.67
.5	.54
.6	.41
.7	.27
.8	.15
0.9	0.05

Figure 6 is a plot of the data in the last three columns of Table III. The full line indicates the absolute temperature, T, of the point P in Figure 5 obtained from the data in Table I. The dotted line represents the solar radiation E_R received, and the broken line the energy E radiated by the moon in cal cm^{-2} min^{-1}.

In general, the fall and rise in temperature lags behind E_R, the energy received by the moon, as might be expected.

The temperature falls from 342° to a value between 200° and 175° K during the first partial phase, and during totality continues to fall slowly, reaching 156° K at the end. For a few minutes after totality the temperature does not change materially, then it rises abruptly during the next 20 minutes. From this it follows that the surface materials of the moon have low heat conductivity.

DISTRIBUTION OF PLANETARY HEAT AND REFLECTED LIGHT ABOUT THE SUBSOLAR POINT

It will now be our purpose to compare the radiation and temperature of the moon as determined from direct observations with

[1] Abbot, *The Sun*, 2d ed., p. 107, 1929.

the thermocouple (Table II) with the values derived theoretically from the solar constant by making suitable allowances for reflected light and conducted heat. Before this can be done the distribution of both reflected light and planetary heat over the hemisphere about the subsolar point must be investigated in much the same manner as we study the distribution of radiation about an electric light. This was accomplished by a continuous series of measurements on the subsolar point made throughout the lunation between first and last quarters in October, 1929.

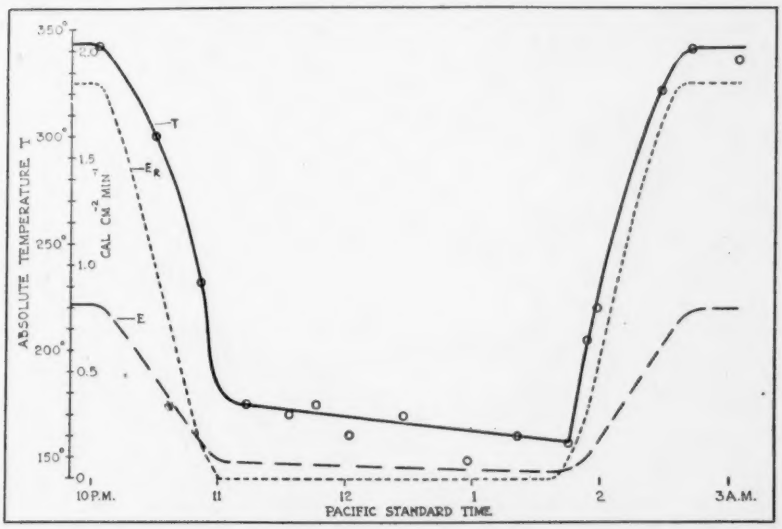

FIG. 6.—March of absolute temperature, T, of energy received from the sun by the moon, E_R, and of energy radiated, E, during the total lunar eclipse of June 14, 1927.

The apparatus employed was a reflecting telescope of 27 inches aperture and 67 inches focal length fed by the coelostat of the Snow telescope.[1] The image of the moon was approximately 15.5 mm in diameter. The deflections, which were of the order of 200 mm for free radiation and 50 mm with the cover-glass, were read visually at intervals during the night. The planetary heat eliminated by the cover-glass and the light transmitted by it were reduced to the zenith by Bouguer's formula in the usual manner.

Simultaneous observations made with the 100-inch telescope at

[1] *Mt. Wilson Contr.*, No. 4; *Astrophysical Journal*, **23**, 6, 1906.

the time of full moon, with suitable comparison stars, furnished the scale of absolute units. The settings of the thermocouple upon the subsolar point were made from the photograph in Plate VIII, upon which were plotted the night-to-night positions of the subsolar

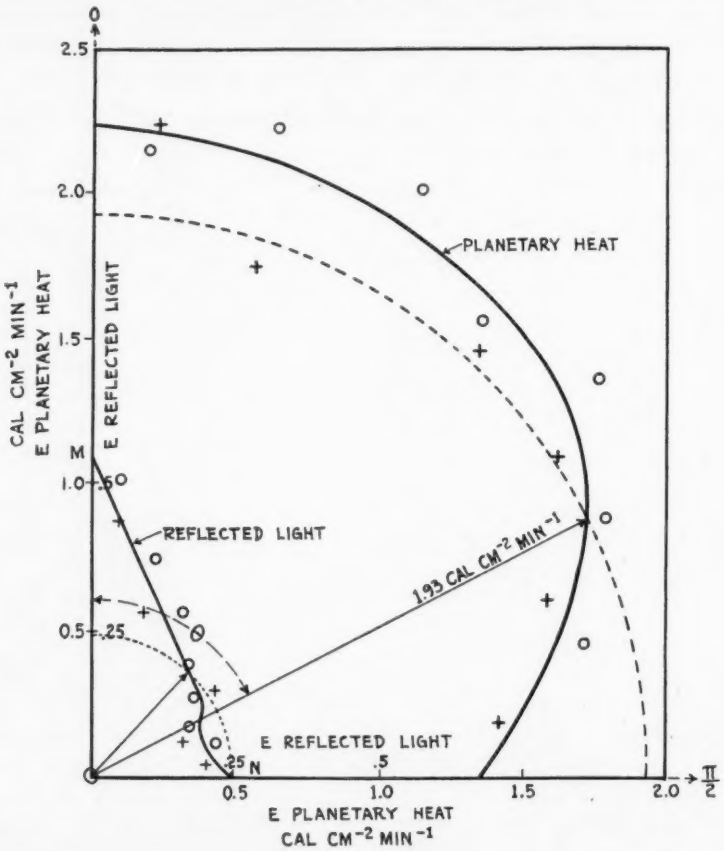

FIG. 7.—Distribution of planetary heat and reflected solar radiation about the subsolar point on the moon.

point. These are shown by the black squares which give the size and position of the thermocouple-receiver for each Greenwich Civil date. The angle between the sun and earth as seen from the subsolar point (which is equivalent to the zenith distance of the earth) was computed by the usual formula. The resulting distribution-curves of planetary heat and reflected light about the subsolar point are

plotted in polar co-ordinates in Figure 7. The intensity scales E on the outside of the figure are for planetary heat and on the inside for reflected light outside the atmosphere and were calibrated by the 100-inch measurements in Table II.

Curiously, the intensities of both planetary heat and reflected light from the subsolar point after full moon (indicated by circles) are somewhat greater than the corresponding intensities before full moon (indicated by crosses). As these observations are all on the subsolar point, this difference can have no relation to accumulation of heat by the moon, which might tend to make the maximum temperature of a fixed point on the surface occur in the lunar afternoon.

It will be noted that the values of the planetary heat E in absolute units at full moon and first quarter in Table II agree with the corresponding values read from the distribution-curve of planetary heat for $\theta=0$ and $\theta=\pi/2$ given in Figure 7. The distribution of reflected light shows a sharp drop from full moon ($\theta=0$) to $\theta=75^\circ$, and a definite increase again near quarter-phase ($\theta=\pi/2$).

Simple considerations show that the mean value of the intensity of both planetary heat and reflected light about the subsolar point is the radius of the hemisphere having the volume generated by revolution of the curves in Figure 7 about the axis $\theta=0$. The arc quadrants of these hemispheres and their radii, which represent the mean spherical intensities, are also shown in Figure 7.

THEORETICAL LUNAR TEMPERATURE

The temperature of the subsolar point on the moon may be computed from the solar radiation received, E_R, if that part of it reflected from the lunar surface, E_r, and that part conducted into it, E_c, are known. The radiated energy E can then be found from the equation

$$E_R-E_r-E_c=E=\eta\sigma T^4\,. \tag{16}$$

Here η is the emissivity, which will be taken as unity in the calculation following. The value of E_R is the solar constant for the times of observation, reduced from the mean distance of the sun to the heliocentric distance of the moon by the inverse-square law. The error in the measurement of this quantity arising from uncer-

tainties in the atmospheric transmission is small, since it depends on atmospheric transmissions principally to the violet of $\lambda\, 3\ \mu$, beyond which there is only about 1 per cent of the solar radiation. These transmissions are easily determined, while those in the region 8–14 μ are determined only with great difficulty.

E_r may be obtained from the average value of m_r° in Table II, which is +3.35 mag. This quantity is the radiometric magnitude of a solid angle of 1 sq. sec. of arc of moonlight from the subsolar point transmitted by the water-cell. Since the energy-curve of moonlight is approximately that of a Ko dwarf star, as has already been pointed out, it would be 0.41 mag. brighter outside the atmosphere; and since the water-cell absorption for a Ko dwarf star is 0.54[1] mag., the radiometric magnitude of 1 sq. sec. of reflected moonlight outside the atmosphere would be +2.40. A similar reduction for the subsolar point at quarter-phase gives +3.13 mag. for a point outside the atmosphere.

From the distribution-curve of reflected light in Figure 7 we find that the mean intensity is 0.85 mag. greater (fainter) than the intensity at full moon, which makes the radiometric magnitude of a square second of reflected moonlight outside the atmosphere +3.25 (mean spherical intensity). This is nearly the observed value at quarter-phase given above, and Figure 7 shows that the actual observed distribution-curve crosses the mean spherical distribution-curve near quarter-phase ($\theta = \pi/2$).

Since the ratio of the whole hemisphere to 1 sq. sec. is −28.57 mag., the magnitude of the total reflected light is −25.32. This, reduced to terms of energy[2] by the equation

$$E_r = 17.3 \times 10^{-12} \times 2.51^{25.32} \text{ cal cm}^{-2} \text{ min}^{-1}, \qquad (17)$$

gives

$$E_r = 0.24 \text{ cal cm}^{-2} \text{ min}^{-1}.$$

The data in Table III may be used to estimate the amount of heat, E_c, conducted into the interior of the moon. Let us assume that before a stable condition, such as existed previous to the eclipse, can be restored, approximately the same amount of heat must be

[1] *Ibid.*, p. 297. [2] *Ibid.*, p. 300.

returned to the moon as was given up by it during the eclipse. Hence, if we interpolate E and E_R from Table III for uniform time-intervals and compute E_c from equation (16), using the temperatures to determine E and various arbitrary values for E_r, until the sum of the values of E_c for the period of the eclipse is zero, we find that to fulfil this condition 52 per cent of the solar energy incident on the area observed must have been reflected, and of the remainder less than 0.1 cal cm^{-2} min^{-1} could have been conducted into the interior of the moon before and after the eclipse. At the subsolar point, where the surface temperature is higher, the conducted heat would be somewhat greater, but even there probably does not exceed 0.1 cal cm^{-2} min^{-1}.

The large value of the reflected light assumed here is borne out by the large fraction of lunar radiation transmitted by the water-cell (0.33) and cover-glass (0.50) shown in Table III, before and after the eclipse.

From the data in Figure 6, Epstein[1] has shown that $(\kappa\rho c)^{-1/2}$, in which κ is the conductivity, ρ the density, and c the specific heat of the lunar crust, is in the neighborhood of 120. This value corresponds to that of pumice or volcanic ash for which the conductivity is about 0.001. This would indicate that at a temperature of 373° K on the moon, the temperature 1 cm below the surface is 100° C. lower, that is, about at the freezing-point of water. It is therefore probably safe to assume that E_c does not exceed 0.1 cal cm^{-2} min^{-1}.

Taking the solar constant on the moon to be 1.95 cal cm^{-2} min^{-1} and applying equation (16), we find

$$\begin{aligned} E &= 1.61 \text{ cal cm}^{-2} \text{ min}^{-1}, \\ T &= 374^\circ \text{ K}. \end{aligned} \tag{18}$$

If E_c is 0.05 cal cm^{-2} min^{-1}, $T = 377°$ K, while if E_c is negligible, $T = 379°$ K.

Since the solar constant probably varies from 1.91 to 1.965 cal cm^{-2} min^{-1}, and the reciprocal square of the heliocentric distance of the moon ranges from 0.962 to 1.039, E_R may vary from 1.84 to

[1] *Physical Review*, **33**, 269, 1929.

2.04 cal cm^{-2} min^{-1}. If we assume that E_r is proportional to E_R and that E_c is practically constant, E varies from 1.52 to 1.69 cal cm^{-2} min^{-1}, and T for the subsolar point would vary from 368° to 378° K.

From the distribution-curve of planetary heat in Figure 7 we find that the mean spherical intensity which is to be compared with the theoretical value in equation (18) is

$$\begin{aligned} E &= 1.93 \text{ cal cm}^{-2} \text{ min}^{-1}, \\ T &= 391^\circ \text{ K}, \\ m'_r &= +1.54 \text{ mag.} \end{aligned} \qquad (19)$$

The planetary heat emitted by the lunar surface is therefore 0.32 cal cm^{-2} min^{-1}, or 20 per cent in excess of that which can be accounted for by the theory, and corresponds to a temperature 17° higher than the solar constant permits after reflection of solar radiation and conducted surface heat on the moon have been deducted.

This result can be explained by any one or by a combination of the following conditions: (1) The solar constant is greater than 1.93 cal cm^{-2} min^{-1}; (2) the emissivity η is greater than unity in the region 8–14 μ; (3) the atmosphere is more transparent in the region 8–14 μ than Fowle's extrapolated coefficients show.

In view of the careful work on the solar constant in spectral regions and under climatic conditions where the atmospheric transmissions which affect the problem are relatively easy to determine, it is hardly possible to allow the increase of 20 per cent necessary to account for the foregoing discrepancy between the theoretical and the observed temperatures of the moon.

As to the second postulate, we have already found, in the section on "Reflection of Solar Radiation of Wave-Length 8–14 μ," evidence that in this region of the spectrum the moon radiates like a black body. The deformation of the energy-curve of the moon necessary to satisfy the observed planetary heat is shown by the dash-and-cross line in Figure 2. We do not regard this deformation as very probable.

This leaves us with the third postulate, which requires that the atmospheric transmissions in the region 8–14 μ be increased about

19 per cent. This can be done easily without seriously encroaching on the transmission-curve for the maximum water-vapor content used in the laboratory determinations and, in view of the large extrapolation from the observed data, would not be regarded as presuming an unreasonable systematic error. Formally then, we compute the magnitude $\Delta m_r'$, which must be added to m_r' in Table I, or to Δm_r, from which m_r' is computed, to make the observed value of T agree with that deduced from the solar constant. To do this it is necessary to assign to the theoretical temperature $T=374°$ K in equation (18) the value $m_r'=1.54$ mag. found from direct measurement in equation (19). The atmospheric transmission-curve in Figure 1 was accordingly symmetrically adjusted between 8 and 14 μ to give this result for a black body at 374° K, and from these data a new set of values of m_r' was computed which appear as corrections, $\Delta m_r'$, to be added to the original values of m_r' in order to make the theoretical and observed temperatures agree. In computing the temperatures of planets with equation (9), $\Delta m_r'$ should be added to m_r' in Table I unless circumstances are found which modify this conclusion.

The effect of $\Delta m_r'$ is to lower the temperature computed from the radiation measurements of Mercury[1] about 45° C., Venus[2] 9°, Mars[3] 10°, and the moon 17°.

REFLECTION OF SOLAR RADIATION FROM THE LUNAR SURFACE

In general, three different theoretical laws of diffuse reflection have been used in discussions of the photometric properties of planets. As applied to apparent solid angles of radiation they are[4]

$$E_1=K_1\cos i \qquad \text{(Lambert)}, \qquad (20a)$$

$$E_2=K_2\frac{\cos i}{\cos i+\cos\theta} \qquad \text{(Lommel-Seeliger)}, \qquad (20b)$$

$$E_3=K_3\frac{\cos i}{\cos\theta} \qquad \text{(Euler)}, \qquad (20c)$$

[1] *Popular Astronomy*, **33**, 299, 1925.

[2] *Ibid.*, **32**, 614, 1924.

[3] *Ibid.*, p. 601, 1924.

[4] Müller, *Photometrie der Gestirne*, p. 68, 1897.

where i is the angle of incidence, θ the angle of reflection, and the K's are constants. We will compare these equations with the observed distribution of reflected light about the subsolar point in Figure 7, and the drift-curve (No. 4 in Figure 3) taken through the water-cell across the full moon.

We may consider the curve of distribution MN about the subsolar point O in Figure 7 to be a straight line. Its intercept N on the axis of $\pi/2$ is 0.46 of the intercept M on the axis of 0°, and since for this curve the angle of incidence i is always zero, the equation which represents it is

$$E' = K_4 \frac{0.46}{0.46 \cos \theta + \sin \theta}. \tag{21}$$

This equation gives us no knowledge as to the effect of varying the angle of incidence i, but we can determine this from drift-curve No. 4 in Figure 3.

The distribution of reflected solar radiation across the disk of the full moon shown in this curve has a general uniform trend, but is high in the middle near the subsolar point, decreases toward the limb, and then rises again at the limb itself. For this curve the values of i and θ are always equal, and their sines are proportional to the abscissae measured from the subsolar point P (Fig. 3). By multiplying E_r' in equation (21) by a power of the secant of a function of i, it may be made to fit both the drift-curve in Figure 3 and the distribution-curve in Figure 7, since i is zero for the latter case. By trial we find that

$$E_r = K \frac{0.46 \sec^2 i/2}{0.46 \cos \theta + \sin \theta} \tag{22}$$

fits both the drift-curve and the distribution-curve fairly well and therefore represents the law of diffuse reflectivity for the moon as derived from these radiometric observations. More complicated functions of i can be found which give better agreement with the observed drift-curve; but as the surface features of the moon probably affect the drift-curve in a manner not entirely dependent on i, such a procedure seems unjustified until more extended observations are obtained.

For $i=0$, equation (22) reduces to the straight line (21) and therefore deviates from the mean curve MN of Figure 7 only in the curved portion of this line. Equation (20*a*) would give a quadrant of a circle of radius OM centered about the origin O. Equation (20*b*) would be a curve intercepting the 0° axis halfway between the origin O and M and the $\pi/2$ axis at a distance from the origin equal to OM. Equation (20*c*) is the locus of a straight line parallel to the axis of $\pi/2$ and passing through M. It is therefore easy to see that equations (20*a*), (20*b*), and (20*c*) do not fit the observed curve at all, while equation (22) agrees fairly well. Table V gives a comparison

TABLE V

INTENSITY OF REFLECTED SUNLIGHT

$i=\theta$	Obs.	Eq. (22)	Eq. (20*a*)	Eq. (20*b*)	Eq. (20*c*)
0°	51	51	50	50	50
15	46	34	48	50	50
30	41	28	43	50	50
45	32	26	35	50	50
60	32	28	25	50	50
75	41	34	13	50	50
90	44	47	0	50	50

of the intensities on an arbitrary scale for various values of $i=\theta$ read from the drift-curve in Figure 3 with those computed from formulae (22), (20*a*), (20*b*), and (20*c*). Here again formula (22) perhaps represents the observations better than formulae (20*a*), (20*b*), and (20*c*.)

RADIOMETRIC MAGNITUDE AND ALBEDO OF THE MOON

Since the radiometric magnitude of a solid angle of 1 sq. sec. of moonlight from the subsolar point at full moon transmitted by the water-cell is +3.35 and the water-cell absorption 0.54 mag., the radiometric magnitude of 1 sq. sec. of reflected full moonlight transmitted by the atmosphere is +2.81. This gives −13.3 for the radiometric magnitude of the reflected light from the whole full moon at mean distance. From the areas under the water-cell and free curves in Figure 3 we find the radiometric magnitude of the whole radiation from the full moon to be −14.8.

The ratio of the solar energy reflected from the subsolar point to that received by it is 0.124. This may be considered as the albedo of the subsolar point but should not be confused with the albedo[1] of the moon, 0.073, which is the ratio of light reflected by the whole hemisphere to that received by it. The albedo, A, may be expressed as

$$A = pq ,$$

where p is the ratio of actual brightness of the moon at full phase to that of a self-luminous body of the same size and position, which radiates as much light from each unit of its surface as the moon receives from the sun under normal illumination, and q is a factor depending on the law of diffuse reflection from the moon. For visual light[2] the value of q is 0.694 and $p = 0.105$. The ratio p for light transmitted by the earth's atmosphere may be obtained from the equation

$$\log p = 0.4[m_r \text{ (sun)} - m_r'' \text{ (moon)}] + \log \pi - 2 \log \sin 1'' .$$

The radiometric magnitude, m_r'', of a solid angle of 1 sq. sec. of the sunlight reflected from the full moon is practically constant over the lunar disk, as may be seen from Figure 3. The mean ordinate of curve No. 4 is 15 per cent lower than at the subsolar point, but since the *maria*, which seem to be responsible for the depressions, cover only one-third of the apparent disk of the full moon, the error in this assumption is probably only 5 per cent, i.e., 0.05 mag. Substituting for m_r'' the value $+2.8$ found above, and for m_r the value -27.18 mag. found for the radiometric magnitude of the sun,[3] we find

$$p = 0.135 ;$$

and if q is the same for all wave-lengths the radiometric albedo of the moon is

$$A = 0.093 .$$

[1] Russell, *Astrophysical Journal*, **43**, 179, 1916.

[2] *Ibid.*

[3] *Mt. Wilson Contr.*, No. 369; *Astrophysical Journal*, **68**, 308, 1928.

TEMPERATURE OF THE DARK SIDE OF THE MOON

Measurements of the radiation from the dark side of the moon 48″ from the east limb were made on July 5, 1927, when this point was nearly opposite the sun on the midnight meridian. The sensitivity used was such that a star of radiometric magnitude 0 would produce 19 mm deflection. Our result was a deflection of 0.09 ± 0.05 mm. This gives radiometric magnitude 10.6 per square second of arc, which corresponds to a temperature of about 120° K. The temperature corresponding to the deflection *plus* its probable error is 125° K, which may be considered its upper limit. Considerable observing will be required to establish a good value of this temperature.

We wish to acknowledge the assistance of Miss Richmond in the rather involved processes of reduction and also in much of the observing program.

CARNEGIE INSTITUTION OF WASHINGTON
MOUNT WILSON OBSERVATORY
December 1929

PRELIMINARY RESULTS OF SPECTROGRAPHIC OBSERVATIONS OF 7 ϵ AURIGAE

By O. STRUVE AND C. T. ELVEY

ABSTRACT

During the eclipse of 7 ϵ Aurigae in 1928–1930 *many absorption lines were unsymmetrical;* in the *beginning* of the eclipse they were *sharp* on the *red side;* in the *middle* of the eclipse they were approximately *symmetrical;* and in the *latter* part of the eclipse they were *sharp* on the *violet side.* Most of the strong lines showed this effect. However, the strong line Mg^+ 4481 and most of the faint lines remained symmetrical throughout the eclipse.

The *absorption lines* were appreciably *strengthened* during eclipse. The line $H\beta$ was found to be *practically black* near the center. In the exact center, however, *there appeared a narrow emission line.*

The *contour of the $H\beta$ line* photographed during the eclipse *agrees* closely *with Unsöld's theoretical curve,* giving for *NHf,* 2.5×10^{17}. The absence of wings suggests that Stark effect is not present, and that the pressure in the reversing layer is very low.

The *radial velocity shows oscillations* having a *period of about 110 days.* These are *independent of the eclipse.* The period is variable from one oscillation to the next, and the amplitude does not remain constant. The shape of the curve is also variable. These oscillations are probably *related to the fluctuations in light* discovered by Stebbins, Frl. Güssow, and McLaughlin.

$H\beta$ and many other strong lines gave *discordant velocities in 1928–1930.* In the first part of the eclipse they gave more positive velocities than the fainter lines, while in the latter part the velocities were much too small, disagreeing completely with Ludendorff's velocity-curve. This effect was well shown by $\lambda\lambda$ 4444, 4468, 4583, etc., and is probably related to the unsymmetrical broadening of these lines. The symmetrical lines, e.g., λ 4481, give radial velocities in good agreement with Ludendorff's curve.

The *variation* in velocity *with a period of 27.1 years* is confirmed. It proceeds in agreement with the predicted curve.

Outside the eclipse there occurred *no appreciable changes in the character of the absorption lines.* Most of them were weaker than during the time of the eclipse. *No trace of the spectrum of the second component* of the long-period binary system could be found at the time of maximum relative velocity (1922–1923).

This star is one of the most interesting objects known to astronomers. In 1903 H. Ludendorff[1] established the fact that its brightness varies with a period of 27.1 years and that the light-curve is that of an eclipsing binary. The radial velocities follow the variations in light and confirm the binary nature of this star.[2] However, observations have established a number of facts that have baffled astronomers for a long time. In the first place, it was shown by Ludendorff that the velocity undergoes variations of a shorter

[1] *Astronomische Nachrichten,* **164,** 81, 1903.

[2] H. Ludendorff, *Sitzungsberichte der Preussischen Akademie der Wissenschaften,* Physikalisch-Mathematische Klasse, 1924, 49.

period, superposed over the long 27-year variation. The shorter oscillations in the velocity-curve are variable in shape and in period, the average being between 140 and 160 days. It is now known from the photometric observations of J. Stebbins, Frl. M. Güssow, and D. B. McLaughlin that the brightness, too, is variable—the oscillations being apparently related to the short-period fluctuations in radial velocity. Certain other phenomena were observed by Vogel and by Eberhard during the eclipse of this star in 1902, but Ludendorff did not succeed in explaining them physically. For details the reader is referred to the original papers of Ludendorff.

The prediction that a new eclipse would begin in 1928 has now been confirmed. The star, whose normal visual magnitude is 3.4, began to decline in light in May or June, 1928, and reached the phase of constant minimum—magnitude 4.2.—about December 1 of the same year. Between December, 1928, and November, 1929, the light has shown only minor fluctuations, attributable, beyond doubt, to the variations of short period. At present the light is again on the increase, and according to expectations normal light will be reached in May, 1930.

In 1917 this star was placed on the regular observing program of the Bruce spectrograph by Director E. B. Frost. Several earlier plates taken by him in 1899 and in 1901 were also available, and some of the earlier results obtained by Frost and Adams were utilized by Ludendorff in his discussion. We have at present at Yerkes a material amounting to over 250 spectrograms. These have all been measured and are now being discussed. In the meantime we wish to report certain very unusual phenomena that have been recorded here during the present eclipse. We hope that this preliminary account of our observations will be of use to other observers in the discussion of their observations, and that it may help in the formation of a physical theory of this strange object.

1. *Asymmetry of lines in 1928–1929.*—The contours of several lines in the spectrum of ε Aurigae were shown at the meeting of the American Astronomical Society in December, 1928, by Elvey.[1] It was noted that the lines were unsymmetrical with the sharp edge toward the red. The ratios of the areas of the violet sides of the

[1] *Popular Astronomy*, **37**, 265, 1929.

lines to the areas of the red sides were taken as a measure of asymmetry. For Ti^+ 4572, which is a typical line, this ratio was 1.2, 1.4, 1.6, 1.2, 1.4, 1.0, and 1.0 on the following dates: April 28, October 29, November 6, 12, 24, December 5 and 9, 1928. The asymmetry was apparently due to a widening of the violet side of the line; the red side remained without change throughout this series. The first plate was taken near the beginning of the eclipse, and the rest near the beginning of constant minimum. A spectrogram taken later in the season, on February 22, 1929, shows that the line Ti^+ 4572 was quite symmetrical. On that date the star was at a minimum in the fluctuations of short period. The two plates taken in December, which also showed symmetrical lines, fell near a maximum. Consequently we believe that the observed asymmetry is not connected with the oscillations of short period.

2. *Asymmetry of lines in 1929–1930.*—When the first spectrogram with a dispersion of three prisms was taken this season, on September 15, 1929, we found that the lines were again unsymmetrical, but in the opposite direction, being sharp on the violet side. All the plates taken since show this phenomenon, but the degree of asymmetry did not remain constant. At the time of this writing the contours are approaching their normal shape, although on January 19, 1930, there was still a small amount of asymmetry present. The ratios of the violet side of Ti^+ 4572 to the red side were 0.7, 0.6, 0.6, and 0.5 on the following dates: October 14, 25, November 22 and 25, 1929. The contours plotted in Figure 1 show that the asymmetry was much more pronounced during the season of 1929–1930 than during the preceding season. The two plates in October were taken just before the star began to increase in light. In fact, Professor Stebbins' light-curve indicates a rather deep minimum in the oscillation of short period for these two dates. The two plates in November were taken after the rise toward maximum had started.

An interesting feature noticed this season was that some of the lines remain symmetrical throughout the series of observations. An inspection of last year's plates indicates that the same lines were also symmetrical in the season of 1928–1929. This is characteristic of nearly all the faint lines, but there are one or two rather strong

lines that also remain symmetrical. This is true of the line Mg^+ 4481, the contours of which are plotted in Figure 2. On October 29, 1928, this line has the appearance of being slightly unsymmetrical and somewhat broader than on the following dates. In general, however, its contour is remarkably constant. For comparison we have shown in Figure 2 the contour of Ti^+ 4468, which is very similar to Ti^+ 4572, except in October, 1929. The contours of Ti^+ 4468 have been

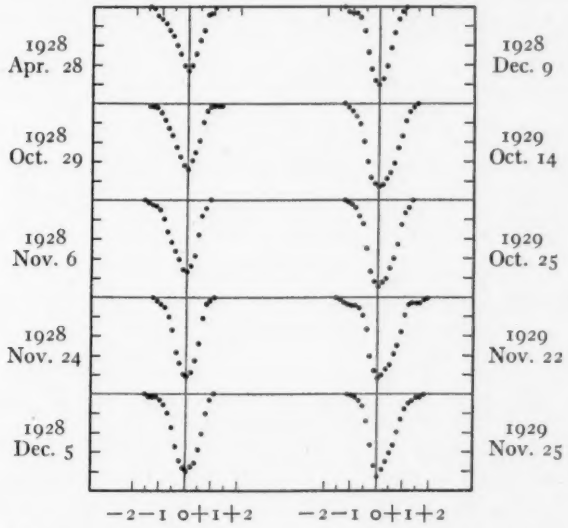

FIG. 1.—Contours of the line Ti^+ 4572 in 7 ε Aurigae. The abscissas are given in Angstrom units; one division in the ordinate corresponds to an absorption of 20 per cent.

plotted in such a way as to show the abnormal displacement of this line with respect to the Mg^+ line. This will be referred to in section 6.

3. *The emission line Hβ.*—On plates taken during the time of the eclipse all absorption lines seem to be stronger than they were before the eclipse started. This is particularly true of $H\beta$, as is well shown on many plates. None of our early spectrograms has been calibrated for the exact photometry of spectral lines, and we are therefore unable to give accurate contours for lines photographed before the beginning of the eclipse. However, we have made a qualitative comparison of plates on which the continuous spectra have equal density. Thus on December 6, 1929, $H\beta$ appears twice

as wide as on August 20, 1927. The earlier plates show an appreciable residual intensity near the center, while the plates taken during eclipse give perfectly black $H\beta$ lines. The metallic lines are also narrower and less deep when taken outside the eclipse.

One of the most interesting changes in the spectrum is the appearance of an extremely fine emission line in the center of the deep absorption line of $H\beta$.[1] This central emission was seen on several

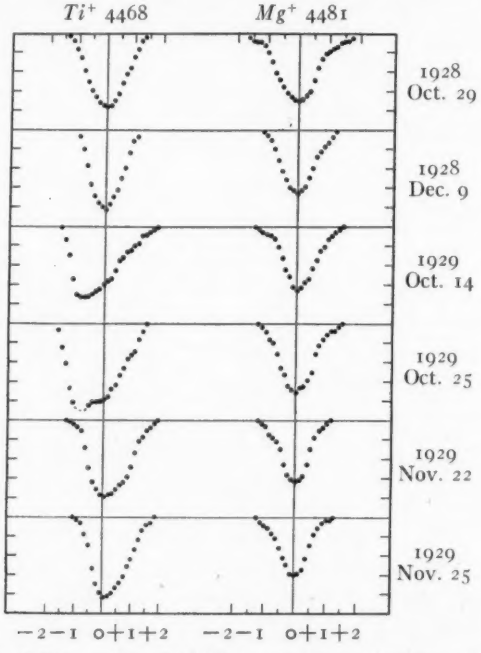

FIG. 2.—Contours of Ti^+ 4468 and of Mg^+ 4481, in 7 ϵ Aurigae. The abscissas are given in Angstrom units; one division in the ordinate corresponds to an absorption of 20 per cent.

plates taken in the fall of 1928 and on most of the plates taken during the present season. We do not find the line on any of our plates taken outside of the eclipse. On our strongest plates $H\beta$ looks as though a section about 0.1 mm wide had been cut out of the continuous spectrum, and in the middle of this region is the faint hairlike emission line. As lines of this character have not been re-

[1] P. Davidovich (*Harvard College Observatory Bulletin*, No. 846, 5. 1927) records a faint emission line on the red side of the $H\beta$ absorption line. We do not find this emission on our plates.

ported previously we thought that the emission line might be due to some spurious effect. It could not be due to instrumental causes. The possibility that it might be due to reflection from the back of the plate was eliminated by the use of backed plates.

At first there was a suspicion that the emission lines might be due to an Eberhard effect. In fact, we were able to produce similar "emissions" in the laboratory. Several wires were stretched across a frame so as to be held just above the emulsion of a plate, which was then exposed to a distant light. The shadows of the wires resembled the spectral absorption lines. Various sizes of wires were used, and one of them was made flat to avoid possible reflections from the emulsions to the back sides of the round wires. In order that the Eberhard effect might be more pronounced the plates were exposed to a faint light producing a general fogging. They were then developed without rocking (to secure the maximum possible effect) in Eastman D-11, regularly used in our spectrographic work. The broader lines showed a rather wide and rounded-off "emission" in the center, and for the artificial line of the same width as the absorption line in ϵ Aurigae, there was a faint trace of a narrow bright line, somewhat similar to that observed in the stellar spectrum. This line was distinctly fainter than the stellar emission line, in spite of the fact that the laboratory conditions had been selected to give the maximum effect. We next made experiments to eliminate completely the Eberhard effect, and found that a five-minute development in a carefully prepared solution of D-11 with thorough rocking was quite effective. The same procedure of development was used for several spectrograms of ϵ Aurigae, on backed plates, and it was found that the emission line was still present. Consequently it would seem that the observed emission line is real.

4. *Contour of the absorption line Hβ.*—We have determined the contour of the absorption line $H\beta$ and have found that it agrees remarkably well with the theoretical contour given by Unsöld. We have computed the contours for various values of NHf, the effective number of atoms, from the equation

$$(\lambda-\lambda_0)^2=NHf\,\frac{2\pi e^4\lambda_0^2}{3m^2c^4}\left(\frac{1-I}{I}\right),$$

where λ is the wave-length of a point on the contour of the line; λ_0, the wave-length of the center of the line; f, the oscillatory strength; N, the number of atoms per cubic centimeter; H, the height of the atmosphere in centimeters; m and e, the mass and charge of the electron; I, the intensity of the point on the contour expressed in percentage of absorption of the continuous spectrum; and c, the velocity of light. The theoretical contours are represented by the

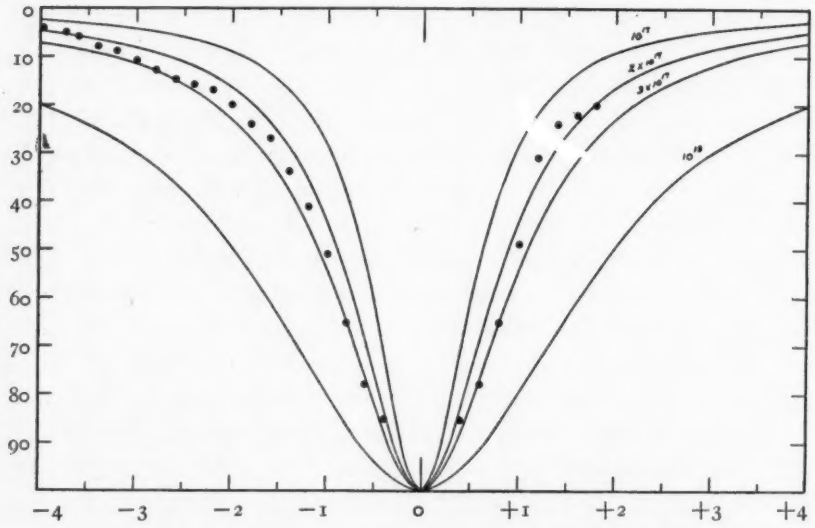

FIG. 3.—Contour of the absorption line $H\beta$ in 7 ϵ Aurigae. The abscissas are given in Angstrom units; one division in the ordinate corresponds to an absorption of 10 per cent. The curves are theoretical contours computed from Unsöld's formula. The observations, representing means from five spectrograms, are shown by dots.

curves in Figure 3, the numbers on the curves being the respective values of NHf. The dots are the mean observations of the contours of five spectrograms. It will be seen that 2.5×10^{17} is about the best value of NHf. If we use for f, 0.12, the value given by Sugiura,[1] we obtain 2.1×10^{18} as the number of atoms in the second quantum state of hydrogen.[2]

[1] *Journal de Physique*, **8**, 113, 1927.

[2] Unsöld has recently corrected an error in his original formula (*Zeitschrift für Physic*, **59**, 367, 1930). Accordingly a slightly different value of f should have been used here. This would not alter the order of magnitude of NH.

UNIV. OF MICH.

PLATE IX

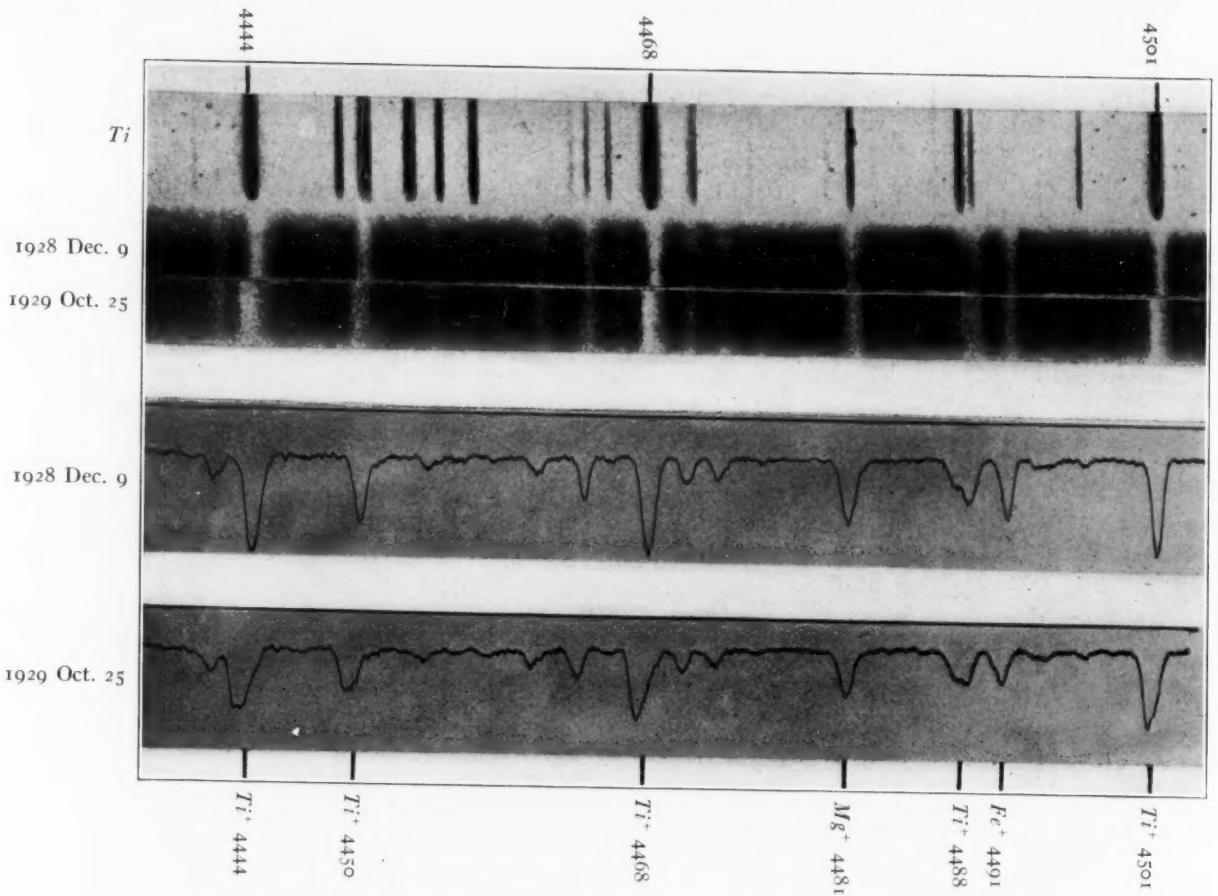

THE SPECTRUM OF 7 ϵ AURIGAE ON DECEMBER 9, 1928, AND ON OCTOBER 25, 1929

So far as is known to us, this is the only star in which the hydrogen lines give satisfactory agreement with theory. Figure 3 shows that the center of the line is practically black, and even our longest exposures fail to show any residual intensity, except for the narrow emission mentioned above. This supports Unsöld's contention that the residual intensities of stellar absorption lines are caused by a mechanism, such as collisions, that becomes important when the pressure is sufficiently great. ε Aurigae is known to be a supergiant,[1] and its atmospheric density must be extremely low, so that collisions between atoms will be very infrequent.

The absence of wings on the hydrogen lines also seems to make the spectrum of this star unique. The usual shape of the observed contour of a hydrogen line is such that if the observations are fitted to a theoretical Unsöld curve, say at a point representing 40 per cent absorption, then the observations which are farther from the center of the line fall below the theoretical curve, excepting at the extremes, where the determinations are quite unreliable. These deviations of the observed contours from the theoretical ones, in the case of hydrogen, we believe to be due to intra-molecular Stark effect. The absence of any appreciable Stark effect in ε Aurigae is doubtless due to its low atmospheric density.

5. *Relative intensities of lines.*—There is some evidence that the relative intensities of certain lines are variable. This may be seen in the tracings of Plate IX. In December, 1928, the ionized iron line λ 4491 was apparently stronger than the blended line marked Ti^+ 4488. This line is really a blend of Ti^+ 4488 and Fe^+ 4489. In October, 1929, the blended line and Fe^+ 4491 were nearly equal in intensity. At present it is difficult to say whether the change in the contour of the blended line is due to an increase in the intensity of the Ti^+ line or to an asymmetry of the Fe^+ line similar to that observed in many other lines.

6. *The radial velocity.*—The velocity determined from $H\beta$ differs from that given by the other lines. In 1928–1929 the hydrogen velocity exceeded that of the mean of all lines, while during the present season it was very much smaller. Sixteen plates taken between July and December, 1929, give an average difference: hydro-

[1] C. H. Payne, *Harvard College Observatory Bulletin*, No. 855, 16, 1928.

gen *minus* mean of all lines, equal to −14.5 km/sec. For 25 plates taken during the season of 1928–1929 the same difference is +6.4 km/sec. In August, 1928, the difference was small. It then increased, reaching a maximum between October, 1928, and February, 1929; thereafter it again decreased, passing through zero in April, 1929. No observations were made during the first part of the summer because of the proximity of the star to the sun. The first plate of the present season was taken on July 29, 1929, and yielded a negative difference, −13.3 km/sec. The maximum negative difference, amounting to −20 km/sec., was observed in September, 1929. Since that time the hydrogen velocity has gradually approached the velocity obtained from the other lines, and at the time of this writing the two values are approximately the same. It will be noticed that the change from positive to negative differences took place about at the time of middle eclipse, but it is peculiar that the positive excess last year was so much smaller than the negative excess observed this season. The peculiarity of the hydrogen line has been noticed also by McLaughlin.[1]

The phenomenon just described is not confined solely to the hydrogen lines. We record a similar behavior for many other lines. In fact, almost all strong lines, chiefly those due to Ti^+ and to Fe^+, show discordant velocities. The effect is best seen when two stellar spectra are placed in juxtaposition, in such a way that the faint absorption lines coincide. This has been done in Plate IX. The upper spectrogram was taken on December 9, 1928, and the lower on October 25, 1929. The faint lines are seen to coincide while many of the strong lines are shifted with respect to one another. A closer examination shows that these shifts are due to unsymmetrical broadening of the stronger lines, though in $H\beta$ this is not the case. The lines Ti^+ 4444, Ti^+ 4468, and Fe^+ 4583 are among those which are shifted by large amounts. As stated above, the stronger lines are generally affected more than the faint lines. This is not always true, however. Thus Mg^+ 4481, which is rather strong, coincides perfectly on the two spectrograms, while the faint line Fe^+ 4491 is apparently shifted. We have not been able to find any very definite regularities for these shifts. Their amounts are not the same, and

[1] *Popular Astronomy*, **38**, 29, 1930.

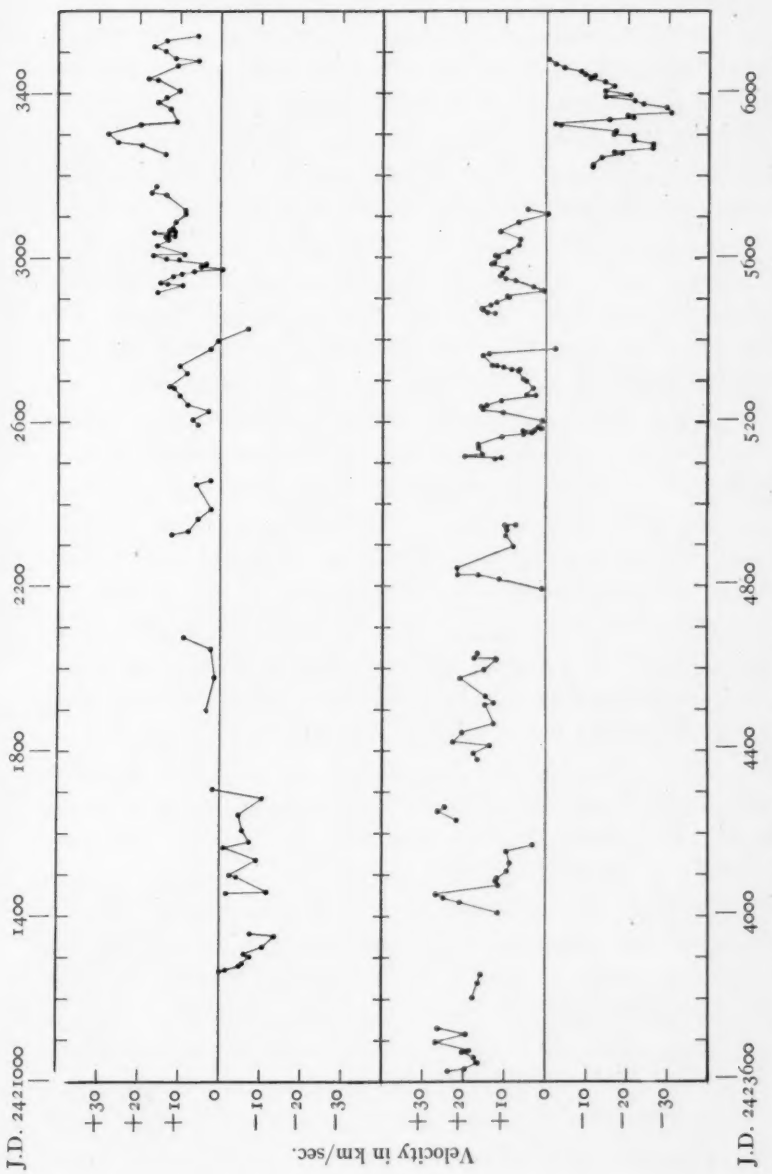

FIG. 4.—Observed radial velocities of 7 ε Aurigae. The upper portion of the curve covers the period from 1917 to 1923; the lower from 1923 to 1930. The values are chiefly based upon measures by Struve. In a later publication all available measures by various persons will be discussed, including spectrograms taken in 1899 and in 1901.

it seems probable that they are caused by a physical agency rather than by a superposition of two spectral components. In the case of such lines as Ti^+ 4444 or Ti^+ 4468, the faint wings of the unsymmetrical lines of October 25, 1929, coincide with the strong central portions of the same lines on December 9, 1928. We are obviously dealing here with the same effect of unsymmetrical broadening that was illustrated in Figure 1 and Figure 2. It seems probable that the unaffected lines, e.g., Mg^+ 4481, give more reliable radial velocities than do the strong Ti^+ and Fe^+ lines which are abnormally shifted. The average difference, Mg^+ 4481 *minus* mean of all lines, was -6.2 for the season 1928–1929, and $+13.1$ during the present season.

According to the prediction of Ludendorff, maximum velocity in the long-period variation should have been reached in 1922 or 1923. This is verified by our observations (Fig. 4). Since then the velocity has gradually declined, in conformity with his velocity-curve. However, during the present season the velocity has been abnormally small, in complete contradiction to the predicted curve. This was not due to the oscillations of short period, since enough observations were secured to correct for them. On the average the radial velocity this season is about 24 km/sec., smaller than last season, while the predicted decline should hardly have exceeded a few kilometers. The discrepancy is doubtless due to the influence of the "affected" lines noted above. Indeed, had we used the $H\beta$ line alone, we would have found a still greater discrepancy. On the other hand, the velocity derived from Mg^+ 4481 would have conformed closely to the predicted curve.

It is of interest to notice that the residuals given in Ludendorff's paper indicate that the same discrepancy took place during the eclipse of 1902. After the middle of that eclipse the velocity was much more negative than required by the curve, while in the beginning of the eclipse it may have been slightly too large. This effect cannot be due to axial rotation of the principal star, since we are here dealing with a broadening of the "affected" lines. The limb-effect noted by Rossitter and by McLaughlin in various other eclipsing binaries requires an unsymmetrical narrowing of all lines.

7. *Oscillations of short period.*—These oscillations in the radial velocity were well marked during the past three years (Fig. 4). All

spectral lines participate in them to the same extent, and all agree in phase. The period seems to have been somewhat shorter than that given by Ludendorff. We find an average value of about 110 days for the past eight cycles. The shape of the curve is not constant, nor does the period hold exactly. The total amplitude ranged from 15 to 22 km/sec. These oscillations seem to be independent of the eclipse.

8. *Character of lines prior to eclipse.*—We have carefully examined our plates taken prior to the eclipse, and have found that the changes in character of the lines are confined to the time of eclipse. There was no appreciable change in the shape of the lines between 1917 and 1928. However, there is some evidence that the radial velocity given by the hydrogen lines did not always coincide with that for the other lines. The differences were invariably much smaller than those recorded for the last two seasons.

In 1922 and 1923 the relative radial velocity of the two components of ε Aurigae was at a maximum. Nevertheless we find no trace of the spectrum of the fainter component.

9. *Velocity and brightness.*—There is some evidence, as was pointed out by McLaughlin, and as is now supported by our measurements, that the short-period variations in velocity are related to the variations in brightness. The minima of the velocity-curve seem to precede the minima of the light-curve by a few weeks, but the observations are too few to establish this beyond doubt. Our comparisons were made with the help of the photo-electric observations of Professor Stebbins at Madison.

10. *Comparison with Potsdam observations.*—It was noted above that the peculiarity in the radial velocities during the time of the present eclipse was similar to that of the eclipse of 1902, as shown by Ludendorff's residuals. It is apparent that the changes are all due to the unsymmetrical broadening of certain lines, and that this broadening is the same effect that was observed by Vogel and Eberhard, and that was later confirmed by Ludendorff. Vogel noted in certain lines a *stufenförmiger Abfall.* This is doubtless the same effect that produces the unsymmetrical broadening of our contours, and that causes the abnormal shifts of certain spectral lines.

11. *Conclusions.*—It seems clear that we are actually dealing with two bodies revolving around one another in a period of 27.1

years. This is demonstrated by the velocity-curve and by the recurrence of the eclipses. Certain deductions concerning the densities of the two components were made by Ludendorff, and are not appreciably altered by our observations. The failure of the secondary spectrum to become visible at the time of maximum separation of the lines is very important, and suggests that one of the two components is either dark (or nearly dark) or that it has a spectrum very different from that of the principal star.

The oscillations of short period in velocity and in light are to be attributed to the primary component. They resemble the variations of certain long-period variable stars and are apparently quite independent of the eclipse.

A very appreciable strengthening of nearly all lines was observed during the time of the eclipse. Inasmuch as no trace of the secondary spectrum was visible in 1922–1923, when the separation should have been a maximum, the observed enhancement of the absorption lines cannot be due to the overlapping of the lines of two spectra. The most natural explanation would be that the number of absorbing atoms is greater at the time of eclipse than outside of it. This probably means that the total thickness of the absorbing layer is increased, without a corresponding increase in the general opacity of the atmosphere. The increased thickness begins rather suddenly, almost in coincidence with the beginning of the eclipse. It is reasonable, therefore, to suppose that it is due to an additional layer of material connected in some way with the secondary component. Ludendorff and McLaughlin have suggested that the secondary may be semi-transparent. This would perhaps account for the presence of the additional thickness of matter, but it would be rather surprising that the increase in intensity of the lines is not greater than it actually is. The total number of atoms determined by Unsöld's method for any one element, say for hydrogen in the second quantum state, is of the order of 10^{18}. This amount of material is quite insignificant in comparison with the total amount of mass in the secondary, known from the radial velocity of the primary. It would be necessary, then, to assume that most of the bulk of the secondary is contained in a form in which it cannot produce selective line absorption. But the small part of the secondary that does produce

line absorption, if spread over the whole volume, would result in so small a density that its state of ionization should be vastly different from that observed for the primary star, and the spectral lines should not be the same. It is rather difficult to avoid this result.

Whatever the origin of the additional layer of absorbing material, it causes unsymmetrical broadening of the lines. It is possible that we are dealing here with a completely new physical phenomenon. Otherwise the broadening must be attributed to Doppler effect, caused by the motion of the additional layer with respect to the original layer of gas. This would not be unreasonable if the additional layer were actually connected with a semi-transparent secondary star. Axial rotation of such a body would account for the facts, but, as we have seen, it is difficult to reconcile the similarity of the two spectra with the low density of a semi-transparent secondary.

We wish to express our thanks to Professor Stebbins for the use of his unpublished light-curve of ε Aurigae. We are also indebted to Professor F. E. Ross and to Dr. G. W. Moffitt for many useful suggestions in connection with the study of the Eberhard effect.

YERKES OBSERVATORY
January 1930

PHOSPHORUS IN STELLAR SPECTRA

By OTTO STRUVE

ABSTRACT

Several *absorption lines* measured in the spectrum of the star 88 γ Pegasi, of spectral class B2, *have been identified with* the strongest lines of *P* III. The existence of these lines in early class B stars is *in agreement with the values of the potentials* of ionization and excitation. The spectrum of *P* I *has no lines* in the photographic region and is therefore unknown in stellar spectra. It is possible that several lines due to *P* II could be found in stars of type A0 or B9.

Phosphorus (atomic number 15) is one of the most abundant elements on the earth. It occupies the twelfth place in the list of chemical elements, constituting about 0.15 of 1 per cent of the total mass of the crust of the earth.[1] Its spectrum has not, to my knowledge, been found in any stellar sources. The absence of phosphorus from the spectrum of the sun has been fully explained by H. N. Russell[2] and by C. E. St. John.[3] The neutral atom of phosphorus produces no lines in the ordinary photographic region of the spectrum.[4] The lines thus far observed in the laboratory are all in the extreme ultra-violet. It is expected, on theoretical grounds, that there may be arc lines in the far infra-red, but these have not yet been observed. The ionization potentials of the phosphorus atom are 10.5, 19.8, and 29.8 volts, for *P* I, *P* II, and *P* III respectively. Consequently we should expect to find the higher stages of ionization represented in the hotter stars. From analogy with the maxima of *Si* and *Al* in their various stages of ionization we conclude that *P* III should be strongest in the early class B stars. The spectral series relationships of the *P* III atom have recently been investigated by R. A. Millikan and I. S. Bowen.[5] They list five lines in the photographic region. Their wave-lengths were taken from the

[1] F. W. Clarke and H. S. Washington, *Proceedings of the National Academy of Sciences*, **8**, 108, 1922.

[2] *Astrophysical Journal*, **70**, 37, 1929.

[3] *Ibid.*, p. 160, 1929.

[4] M. O. Saltmarsh, *Philosophical Magazine*, **47**, 874, 1924.

[5] *Physical Review*, **25**, 600, 1925.

work of P. Geuter.[1] The only other set of accurate wave-lengths of phosphorus is contained in the well-known tables of Exner and Haschek.[2]

The stellar wave-lengths given in Table I were measured in the spectrum of the star 88 γ Pegasi, of spectral class B2. The linear dispersion of the plate was 30 A per millimeter at λ 4500. The lines are faint and rather difficult to measure; but they are sufficiently strong to leave no doubt of their reality. It will be seen that the

TABLE I

LINES OF *P* III

LABORATORY WAVE-LENGTHS IN I.A. (AIR)		STAR	REMARKS
Geuter	Exner and Hascheck		
4057.39 (4)....	4057.4	.....	Too faint
4059.27 (6)....	4059.50	4060.71 (2)	
4080.04 (7)....	4080.23	4080.09 (1)	
4222.15 (7)....	4222.17	4222.33 (2)	
4246.68 (7)....	4246.6	4246.6 (1)	Uncertain

agreement is very satisfactory for the last three lines. The first line is too faint to be represented in the star. The second line is doubtless a blend with the two lines of *O* II, λ 4060.58 and λ 4060.98. This explains also the abnormal stellar intensity of this line. The other intensities agree well with the laboratory values.

It would seem that the evidence in favor of the identification with *P* III is as satisfactory as could be desired. Stars of early spectral class contain comparatively few lines, and it is not very probable that the coincidences are due to chance. The lines are so faint that it is rather difficult to trace them in other stars.[3] Apparently they reach maximum intensity at or near class B2.

The spectrum of *P* II has been partially analyzed by Bowen.[4] Several fairly strong lines are in the photographic region, but none

[1] Dissertation, Bonn, 1906; *Zeitschrift für wissenschaftliche Photographie*, **5**, 1, 1907; Kayser, *Handbuch der Spectroscopie*, **6**, 247, 1912.

[2] *Die Spektren der Elemente bei normalem Druck*, **3**, 172, 1912.

[3] They were observed also in ζ Persei (B1) and ζ Cassiopeiae (B3).

[4] *Physical Review*, **29**, 510, 1927.

has been found in the stars. F. E. Baxandall's careful measurements in stars of class B8–Ao give no satisfactory coincidences with the laboratory wave-lengths. However, it is not impossible that some of the lines of *P* II could be located by means of high-dispersion spectrograms of such stars as α Cygni or β Orionis.

The astrophysical behavior of phosphorus appears to be very similar to that of the two preceding elements in the periodic table, *Al* (13) and *Si* (14), and of the element following it,[1] i.e., *S* (16). All of them come to a maximum in the earliest subdivisions of class B, displaying the spectra of their doubly ionized atoms.

YERKES OBSERVATORY
March 7, 1930

[1] A study of *S* III and of *S* II in stellar spectra is now being undertaken by Mr. F. E. Roach at the Yerkes Observatory.